

New Aspects of Invasive Growth Regulation Identified by Functional Profiling of MAPK Pathway Targets in *Saccharomyces cerevisiae*

Matt D. Vandermeulen and Paul J. Cullen¹

Department of Biological Sciences, University at Buffalo, New York 14260-1300

ORCID ID: 0000-0002-6703-1480 (P.J.C.)

QA1

ABSTRACT MAPK pathways are drivers of morphogenesis and stress responses in eukaryotes. A major function of MAPK pathways is the transcriptional induction of target genes, which produce proteins that collectively generate a cellular response. One approach to comprehensively understand how MAPK pathways regulate cellular responses is to characterize the individual functions of their transcriptional targets. Here, by examining uncharacterized targets of the MAPK pathway that positively regulates filamentous growth in *Saccharomyces cerevisiae* (fMAPK pathway), we identified a new role for the pathway in negatively regulating invasive growth. Specifically, four targets were identified that had an inhibitory role in invasive growth: *RPI1*, *RGD2*, *TIP1*, and *NFG1/YLR042c*. *NFG1* was a highly induced unknown open reading frame that negatively regulated the filamentous growth MAPK pathway. We also identified *SFG1*, which encodes a transcription factor, as a target of the fMAPK pathway. *Sfg1p* promoted cell adhesion independently from the fMAPK pathway target and major cell adhesion flocculin *Flo11p*, by repressing genes encoding presumptive cell-wall-degrading enzymes. *Sfg1p* also contributed to *FLO11* expression. *Sfg1p* and *Flo11p* regulated different aspects of cell adhesion, and their roles varied based on the environment. *Sfg1p* also induced an elongated cell morphology, presumably through a cell-cycle delay. Thus, the fMAPK pathway coordinates positive and negative regulatory proteins to fine-tune filamentous growth resulting in a nuanced response. Functional analysis of other pathways' targets may lead to a more comprehensive understanding of how signaling cascades generate biological responses.

KEYWORDS filamentous growth; transcription; expression profiling; fungal pathogens; adhesion

SIGNAL transduction pathways mediate cellular responses, which can include the response to stress, cell differentiation, and morphogenetic changes. One type of signaling pathway that functions in eukaryotes as a driver of development and stress responses are mitogen-activated protein kinase (MAPK) pathways, which regulate transcription factors that modify gene expression to induce a cellular response (Seger and Krebs 1995; Madhani *et al.* 1999; Chang and Karin 2001; Zeitlinger *et al.* 2003; Seger 2010; Morrison 2012). Because transcription factors can have many transcriptional targets, the individual functions of all targets must

be considered to understand the complete phenotype of a signaling pathway. Thus, characterizing the transcriptional targets of a MAPK pathway may lead to new understandings in the regulation of biological responses.

In the budding yeast *Saccharomyces cerevisiae*, the filamentous growth MAPK (fMAPK) pathway is one of multiple pathways that regulates the cellular response to nutrient limitation known as filamentous growth (Carlson *et al.* 1981; Gimeno *et al.* 1992; Lorenz and Heitman 1998; Pan and Heitman 1999, 2000; Cullen and Sprague 2000, 2012; Crespo *et al.* 2002; Lamb and Mitchell 2003; Borneman *et al.* 2006; Chavel *et al.* 2010, 2014; González *et al.* 2017; Norman *et al.* 2018; Mutlu *et al.* 2019; Brito *et al.* 2020). Filamentous growth occurs in many fungal species, and, in pathogenic fungi, such as the human pathogen *Candida albicans*, it is critical for virulence, making filamentous growth an important aspect of fungal biology (Lo *et al.* 1997; Wendland 2001; Nobile *et al.* 2006; Sohn *et al.* 2006; Labbaoui *et al.* 2006).

Copyright © 2020 by the Genetics Society of America

doi: <https://doi.org/10.1534/genetics.120.303369>

Manuscript received May 20, 2020; accepted for publication July 7, 2020; published Early Online July 14, 2020.

Supplemental material available at figshare: <https://doi.org/10.25386/genetics.12609710>.

¹Corresponding author: Department of Biological Sciences, State University of New York at Buffalo, 532 Cooke Hall, Buffalo, NY 14260-1300. E-mail: pjculen@buffalo.edu

75 2017; Zhao *et al.* 2018; Brito *et al.* 2020). Filamentous
76 growth involves a switch from yeast-form growth (round cell
77 morphology) to filamentous-form growth, where cells pro-
78 duce filament-like structures. The filament-like structures re-
79 sult from three major changes to the cell: an increase in cell
80 length, a reorganization of cell polarity, and increased cell-to-
81 cell adhesion (Roberts and Fink 1994; Cullen and Sprague
82 2012). Filamentous growth causes cells to invade into sub-
83 strates, a behavior called invasive growth (Roberts and Fink
84 1994). Invasive growth is presumed to be a scavenging re-
85 sponse for cells to search for nutrients because it is mainly
86 induced by nutrient limitation, such as fermentable carbon
87 source (Cullen and Sprague 2000, 2012) and nitrogen
88 (Gimeno *et al.* 1992) limitation. It can also be induced by
89 high cell density through quorum sensing molecules (Chen
90 and Fink 2006; González *et al.* 2017; Lenhart *et al.* 2019).
91 When cells adhere and invade together in high cell density,
92 they can form a gouge into surfaces, which is called aggregate
93 invasive growth (Chow *et al.* 2019a).

94 The fMAPK pathway controls the activity of transcription
95 factors that include Ste12p and Tec1p [Figure 1A, (Gimeno
96 *et al.* 1992; Gimeno and Fink 1994; Borneman *et al.* 2006;
97 Heise *et al.* 2010; Cullen and Sprague 2012; van der Felden
98 *et al.* 2014)]. These proteins induce the expression of many
99 target genes (Madhani *et al.* 1999; Roberts *et al.* 2000; Heise
100 *et al.* 2010; Adhikari and Cullen 2014; van der Felden *et al.*
101 2014; Chow *et al.* 2019b; Zhou *et al.* 2020). Several highly
102 induced targets of the fMAPK pathway positively regulate
103 filamentous growth, such as *BUD8*, which encodes a protein
104 involved in bud-site-selection at the distal pole [Figure 1A,
105 (Zahner *et al.* 1996; Taheri *et al.* 2000; Ni and Snyder 2001;
106 Cullen and Sprague 2002)]; *FLO11*, which encodes the major
107 cell adhesion mucin-like flocculin [Figure 1A, (Lambrechts
108 *et al.* 1996; Lo and Dranginis 1996, 1998; Madhani *et al.*
109 1999; Rupp *et al.* 1999; Guo *et al.* 2000; Cullen and
110 Sprague 2012)]; and *CLN1*, which encodes a G₁ cyclin
111 (Hadwiger *et al.* 1989), whose induction leads to a delay in
112 the cell cycle resulting in an elongated cell morphology [Fig-
113 ure 1A, (Loeb *et al.* 1999; Madhani *et al.* 1999)]. Many other
114 transcriptional targets remain uncharacterized, raising the
115 possibility that the fMAPK pathway may have unappreciated
116 roles in regulating filamentous growth.

117 A longstanding problem surrounding fMAPK pathway tar-
118 gets has been identifying phenotypes. One reason may be that
119 some genes have a phenotype only noticeable under some
120 conditions. Another reason is that targets might only contrib-
121 ute to a phenotype in a small way, if the cumulative effect of
122 many genes is required to produce a phenotype. This means
123 that some targets might have subtle phenotypes that could be
124 overlooked. By examining cells lacking individual fMAPK
125 pathway target genes under a variety of conditions for subtle
126 but reproducible phenotypes, we identified new roles for five
127 fMAPK pathway targets. One unexpected discovery that came
128 from this approach was that the fMAPK pathway, which
129 positively regulates invasive growth, can also negatively reg-
130 ulate aspects of invasive growth under some conditions. The

other unexpected finding came from the characterization of a
131 newly identified target, the transcription factor *SFG1* (Fujita
132 *et al.* 2005; White *et al.* 2009), which enabled the fMAPK
133 pathway to regulate cell adhesion and the cell cycle by mul-
134 tiple mechanisms. Our study suggests that these new func-
135 tions for the fMAPK pathway provide an additional level of
136 versatility, which presumably allows for more nuanced re-
137 sponses in different environments. Therefore, characterizing
138 the targets of a signaling pathway can lead to new insights
139 about how pathways regulate biological responses.

Materials and Methods

Yeast strains and plasmids

Yeast strains are listed in Table 1. Gene deletions were made
144 through homologous recombination, constructed using auxo-
145 trophic or antibiotic resistance markers amplified by poly-
146 merase chain reaction (PCR) and introduced into yeast by
147 lithium acetate transformation as described (Gietz 2014).
148 Primers for PCR are listed in Supplemental Material, Table
149 S1. Strains were verified by PCR southern analysis and phe-
150 notype, when possible. All strains are isogenic with HYL333
151 of the Σ 1278b background [provided by G. Fink, Whitehead
152 Institute for Biomedical Research, Cambridge, MA, (Liu *et al.*
153 1993)]. pRS316 plasmid is a control vector containing *URA3*
154 as described in Sikorski and Hieter (1989) for experiments
155 that use *ura*⁻ strains. Yeast extract, peptone, dextrose (YPD)
156 medium was used at the concentration of glucose specified
157 (2%, 10%, 16%). For high osmolarity medium, sorbitol
158 (sorb) is added to YPD medium (2% Glu + 8% Sorb).
159 YP-GAL (2%), YPD medium except 2% galactose is used in-
160 stead of dextrose. Synthetic complete medium (yeast nitro-
161 gen base without amino acids, dextrose (2%) or galactose
162 (2%), amino acids) was also used. SD+AA, synthetic media
163 with dextrose and amino acids; SD-URA, synthetic media
164 with dextrose and amino acids minus uracil. SGAL-URA, syn-
165 thetic medium with galactose and amino acids minus uracil.
166 SLAD, synthetic low ammonium, dextrose (2%) (Gimeno
167 *et al.* 1992).

Analysis of RNA sequencing data

RNA sequencing (RNAseq) analysis was previously performed
172 in Adhikari and Cullen (2014). Here, the RNAseq data were
173 visualized in a volcano plot generated using the program Instant
174 Clue (<http://www.instantclue.uni-koeln.de/>). The plot
175 was cropped to show targets induced by fMAPK (genes with a
176 negative-fold change in the *ste12Δ* mutant).

Microscopy

For DIC (differential interference contrast) imaging, a Zeiss
180 Axioplan 2 microscope (Oberkochen, Germany) was used.
181 The digital images were acquired with an Axiocam MRm
182 camera (Zeiss). For image acquisition and analysis, Axiovision
183 4.4 software (Zeiss) was used.

131 132 133 134 135 136 137 138 139 140 141 142 143 144 145 146 147 148 149 150 151 152 153 154 155 156 157 158 159 160 161 162 163 164 165 166 167 168 169 170 171 172 173 174 175 176 177 178 179 180 181 182 183 184 185 186

187
188
189
190
191
192
193
194
195
196
197
198
199
200
201
202
203
204
205
206
207
208
209
210
211
212
213
214
215
216
217
218
219
220
221
222
223
224
225
226
227
228
229
230
231
232
233
234
235
236
237
238
239
240
241
242

Plate-washing assay

The plate-washing assay was used to visualize differences in filamentous growth between the wild-type strain and mutants (Roberts and Fink 1994; Cullen 2015). Briefly, cells were spotted on medium as indicated at 30° for 1–10 days. Cells were spotted equidistant to each other and the edge of the plate to ensure uniform growth. Plates were placed under a stream of water, and colonies were rubbed gently by hand to remove noninvasive cells. Cells that remained in the agar after washing were considered to be part of the invasive scar. Images of the invasive scars were captured by ChemiDoc XRS+ molecular imager (from Bio-Rad Laboratories, Hercules, CA) under immunoblot/chemicoloric setting with no filter or a Nikon D3000 (Nikon, Garden City, NY) digital camera after the plate wash.

To quantify invasive growth, images from the plate-washing assay were imported into ImageJ (National Institutes of Health, Bethesda, MD; <https://imagej.nih.gov/ij/>). Each image was inverted and treated with identical parameters for adjusting brightness and contrast. For each image, the background was subtracted. Using the set threshold tool with light background set, a threshold was set to convert the invasive scars into pixel images. The threshold was set so that the area around the scar was excluded and areas of invasive growth were highlighted. The pixel area of each invasive scar was measured by the analyze particles tool. This was performed again for ~~a~~ two additional higher thresholds (*i.e.*, 10, 30, and 50). The measured values from the three different threshold settings were totaled for a final value. Significance was determined for three replicates, separately for each type of media.

To quantify an invasive growth pattern, images of washed colonies were cropped to 350 × 350 pixels, inverted, and imported into ImageJ. Each image was treated with identical parameters for adjusting brightness and contrast. Images had their background subtracted with a value of 10,000 particles. A box was drawn across the midsection of the image with a pixel height of 40. Using the plot profile tool, which measures the gray value for pixels, a plot profile was generated for each strain of this region of the invasive scar and overlaid onto a graph in excel.

Measuring cell adhesion in liquid and from cells grown on semisolid agar media

To analyze cell adhesion in liquid media, cells were grown for 24 hr in YP-GAL (2%) media at 30°. Images were captured at 5× by microscopy and imported into ImageJ. The background was subtracted by 50 particles. A threshold was applied, set to 170, to convert the image into a binary pixel image. A scale of 1.266 μm per pixels was applied. Using the analyze particles tool, the area of cell clusters was measured and averaged. The averages of three replicates were used to calculate significance. Cells behaved the same if imaged directly in media or after being washed with water.

To analyze cell adhesion on semisolid media, cells were grown for 16 hr in SD+AA at 30°, washed in dH₂O, and cells were spotted onto YP-GAL (2%) medium. Plates were incubated at 30° for 3 days. Cells were harvested from colonies using a metal spatula with care not to excise the agar. Cell biomass was determined by weight. Cells were resuspended in 20 ml dH₂O in 50 ml conical tubes. Tubes were inverted vigorously by hand 10 times. The contents of the tube were poured into a Petri dish, and particles were photographed by ChemiDoc XRS+ molecular imager under immunoblot/chemicoloric setting with no filter. Images were imported into the GIMP2 program and cropped by 970 × 970 pixels circularly. The background was subtracted by 50.0 particles. A threshold was applied, set to 10, to generate a binary pixel image. Images were imported into ImageJ. A scale of 970 pixels = 82.13 mm based on measurements from the ChemiDoc XRS+ molecular imager and GIMP2 program (verified with ruler) was set. Using the analyze particles tool, the total area of cell adhesion was measured. Significance was determined for three replicates.

Colony immunoblots for *Flo11p* shedding

Colony immunoblots were performed as described (Karunanithi *et al.* 2010). Cells were grown in 3 ml SD+AA for 16 hr. Cells were pelleted and washed with dH₂O and spotted onto a nitrocellulose membrane directly on top of YP-GAL (2%) orYPD (2% Glu) plates. Plates were incubated at 30° for 3 days. Cells were washed off of the nitrocellulose by plate-washing. The nitrocellulose membrane was examined by immunoblot analysis with anti-HA antibodies and imaged by ChemiDoc XRS+ molecular imager. Signal intensity was measured with the volume tool in Image Lab (<https://www.bio-rad.com/en-us/product/image-lab-software?ID=KRE6P5E8Z>). Wild-type values were set to 1. Significance was determined for three replicates.

Biofilm/mat assays

Biofilm/mat assays were performed as described (Reynolds and Fink 2001; Karunanithi *et al.* 2012). Cells were grown in SD+AA for 16 hr and spotted onto semisolid agar (0.3%) medium for 3 days. To analyze plastic adhesion, cells were spotted onto YP-GAL (2%) plates and incubated at 30° for 3 days. Cells were then removed from the agar using a toothpick, resuspended in water, and adjusted to an optical density of A₆₀₀ = 1.3. Aliquots (100 μl) of cell suspensions were added to polystyrene wells (96-well Falcon Microtest Tissue culture plate) and incubated for 4 hr. An equal volume of 1% crystal violet dye (DIFCO) was added to each well for 20 min. Wells were washed five times and photographed. Quantification was performed with ImageJ. Each well was circularly cropped 250 × 250 pixels from the center of the well. A threshold of 120 was set, then the analyze particle tool measured the total pixel area. Wild-type values were set to 1. Significance was determined for three replicates.

243
244
245
246
247
248
249
250
251
252
253
254
255
256
257
258
259
260
261
262
263
264
265
266
267
268
269
270
271
272
273
274
275
276
277
278
279
280
281
282
283
284
285
286
287
288
289
290
291
292
293
294
295
296
297
298

299 **Comparative protein and gene sequence assessments**

300 Comparative assessments for *Nfg1p*, *Rgd2p*, *Rpi1p*, *Tip1p*,
301 and *Sfg1p* protein sequences were performed by BLAST
302 (<https://blast.ncbi.nlm.nih.gov/Blast.cgi>). Nonredundant
303 protein sequences (nr) was set for database. The algorithm
304 was blastp (protein–protein BLAST). Sequences used were
305 from the reference strain (S288c) downloaded from the
306 *Saccharomyces* Genome Database (SGD) (<https://www.yeastgenome.org/>). Comparative assessment of syn-
307 tency for *SFG1* was performed with the Yeast Gene Order
308 Browser [<http://ygob.ucd.ie/>], (Byrne and Wolfe 2005,
309 2006)].

310 **Quantitative reverse transcription PCR**

311 Quantitative reverse transcription PCR (RT-qPCR) was used
312 to measure the relative expression of *FLO11* in wild type with
313 pRS316 and the *nfg1Δ*, *rgd2Δ*, *rpi1Δ*, *tip1Δ*, *ste12Δ*, and
314 *dig1Δ* mutants. Cells were spotted onto YPD (10% Glu)
315 and incubated at 30° for 2 days. Cells were scraped from
316 the surface of the agar, washed in 1 ml dH₂O, and harvested
317 by centrifugation. RT-qPCR was also used to measure the
318 relative expression of *FLO11*, *DSE1*, *DSE2*, *DSE4*, and
319 *SCW11* in wild type and the *sfg1Δ* mutant. Cells were grown
320 in 5 ml YPD (2% Glu) cultures grown at 30° for 23 hr. YPD
321 (1.5 ml) (2% Glu) was pelleted and washed with 1 ml dH₂O;
322 a 100 μl aliquot of washed cells was pipetted into 2 ml liquid
323 YP-GAL (2%) cultures and incubated at 30° with shaking for
324 32 hr. After 32 hr, 2 ml of each sample was washed with
325 1 ml dH₂O and harvested by centrifugation. RT-qPCR was
326 also used to verify targets of the fMAPK pathway by measur-
327 ing the relative expression of *NFG1*, *RGD2*, *RPI1*, *TIP1*, and
328 *SFG1* in wild type and the *ste12Δ* mutant. Cells were grown in
329 5 ml YPD (2% Glu) cultures grown at 30° for 16 hr; 1.5 ml
330 of 16 hr cultures were pelleted and washed with 1 ml dH₂O.
331 A 100 μl aliquot of washed cells was pipetted into YP-GAL
332 (2%) liquid medium and incubated for 5.5 hr at 30°, washed
333 with 1 ml dH₂O, and harvested by centrifugation. Cells not
334 immediately used in RNA extractions were stored at -80°.

335 RNA was harvested by hot-acid phenol–chloroform extrac-
336 tions as described (Adhikari and Cullen 2014). Samples were
337 further purified using a QIAGEN RNeasy Mini Kit (catalog
338 number 74104; QIAGEN, Valencia, CA). RNA purity and con-
339 centration was measured with NanoDrop (NanoDrop 2000C;
340 Thermo Fisher Scientific, Waltham, MA). RNA stability was
341 determined by agarose gel electrophoresis. cDNA was gener-
342 ated and RT-qPCR was performed as previously described
343 (Chow et al. 2019b). cDNA was generated using iScript Re-
344 verse Transcriptase Supermix (catalog number 1708841;
345 Bio-Rad). RT-qPCR was performed using iTaq Universal
346 SYBR Green Supermix (catalog number 1725121; Bio-Rad)
347 on the Bio-Rad CFX384 Real Time System. Primers were
348 obtained from Sigma (Sigma Chemical, St. Louis, MO).
349 Primer sequences can be found in Table S2. *ACT1* housekeep-
350 ing gene primers were based on Chow et al. (2019b). Primer
351 sequences used for *FLO11* were based on Chen and Fink
352

353 (2006). All starting gene concentrations were normalized
354 to the housekeeping gene *ACT1* (Chavel et al. 2010;
355 González et al. 2017). Relative gene expression was calcu-
356 lated using the 2- Δ Ct formula; Ct was defined as the cycle
357 where fluorescence was statistically significant above back-
358 ground (González et al. 2017); ΔCt is the difference in Ct
359 between a target gene and the housekeeping gene (*ACT1*;
360 González et al. 2017). RNA was prepared from three biolog-
361 ical replicates. Average values are reported.

362 **Measurement of fMAPK pathway activity**

363 To analyze fMAPK pathway activity by the β-galactosidase
364 (*lacZ*) assay, cells were grown in synthetic medium (SD-URA)
365 for 16 hr. Cells were washed once in dH₂O and resuspended
366 in the medium indicated for 4.5–6.5 hr of growth. Cells were
367 harvested by centrifugation and stored at -80°. The *lacZ*
368 assays were then performed as described (Jarvis et al.
369 1988; Cullen et al. 2000) using a *FUS1-lacZ* reporter as the
370 readout of fMAPK pathway activity. To analyze fMAPK path-
371 way activity by the *FUS1-HIS3* transcriptional (growth) re-
372 porter, strains were spotted onto SD-HIS+ATA (3-amino-
373 1,2,4-triazole) medium and observed for growth after
374 3 days.

375 To analyze fMAPK pathway activity by phosphoblot anal-
376 ysis, cells were grown to saturation in SD-URA medium. Cells
377 were washed and inoculated in 5 ml SD-URA for 5.5 hr at
378 30°. Cell extracts were prepared for immunoblot analysis
379 according to established procedures (Lee and Dohlman
380 2008; Adhikari and Cullen 2014). Proteins were precipitated
381 by trichloroacetic acid (TCA). Cells were lysed in TCA buffer
382 (10 mM Tris-HCl pH 8.0; 10% TCA; 25 mM ammonium
383 acetate; 1 mM EDTA) containing glass beads by vortexing
384 for 1 min then placing on ice for 1 min five times. Cells were
385 centrifuged at 15,000 × g for 10 min at 4° and the pellet
386 was mixed in 150 μl of resuspension buffer (0.1 M Tris-HCl
387 pH 11.0; 3% SDS) and boiled for 5 min at 95°. Samples
388 were centrifuged at 15,000 × g for 5 min; 10 μl of each
389 sample was used to measure protein concentration using
390 Pierce BCA Protein Assay Kit (catalog# 23225; Thermo Scien-
391 tific). An equal volume of 2× sodium dodecyl sulfate
392 (SDS) loading dye (100 mM Tris-HCl pH 6.8; 4% SDS;
393 0.2% Bromophenol Blue; 20% glycerol; 200 mM
394 β-mercaptoethanol) was added to the supernatant. Protein
395 samples were separated on 10% SDS polyacrylamide gels
396 (SDS-PAGE) and transferred to nitrocellulose membranes
397 (Amersham Protran Premium 0.45 μm NC; GE Healthcare
398 Life Sciences). The membrane was blocked in immunoblot
399 buffer [5% nonfat dry milk (for *Pgk1p* and *Kss1p*) or 5%
400 bovine serum albumin (BSA) (for P~*Kss1p*), 10 mM Tris-
401 HCl (pH 8), 150 mM NaCl, and 0.05% Tween 20] for
402 16 hr at 4° rocking. Radiance Plus Chemiluminescent sub-
403 strate from Azure Biosystems (Dublin, CA) was used for de-
404 tection. Mouse α-*Pgk1p* antibodies (#459250; Thermo
405 Fisher Scientific, Rockford, IL) were used to detect *Pgk1p*
406 as a loading control. Secondary antibodies, goat α-mouse
407 (#170-6516; Bio-Rad Laboratories), were used to detect
408

primary antibodies (*Pgk1p*) for 1 hr at 20° with rocking. Phosphorylated *Kss1p* was detected by p42/p44 antibodies (#4370; Cell Signaling Technology, Danvers, MA) and total *Kss1p* was detected using α-*Kss1p* antibodies (#6775; Santa Cruz Biotechnology, Santa Cruz, CA). Secondary antibodies, goat anti-rabbit IgG-HRP (#111-035-144; Jackson Immuno-Research Laboratories, West Grove, PA), were used to detect primary antibodies (*Kss1p* and P~*Kss1p*) and incubated for 1 hr at 20° with rocking. The blot was imaged by ChemiDoc XRS+ molecular imager. Signal intensity was measured by using the volume tool in Image Lab (<https://www.bio-rad.com/en-us/product/image-lab-software?ID=KRE6P5E8Z>).

Data availability

The authors state that all data necessary for confirming the conclusions presented in the article are represented fully within the article. Strains and plasmids are available upon request. The Gene Expression Omnibus (GEO) accession number for the previously reported expression profiling data are GSE61783 (Adhikari and Cullen 2014). Supplemental material is available at FigureShare: link to be provided. Supplemental material available at figshare: <https://doi.org/10.25386/genetics.12609710>.

Results

Characterizing transcriptional targets of the fMAPK pathway

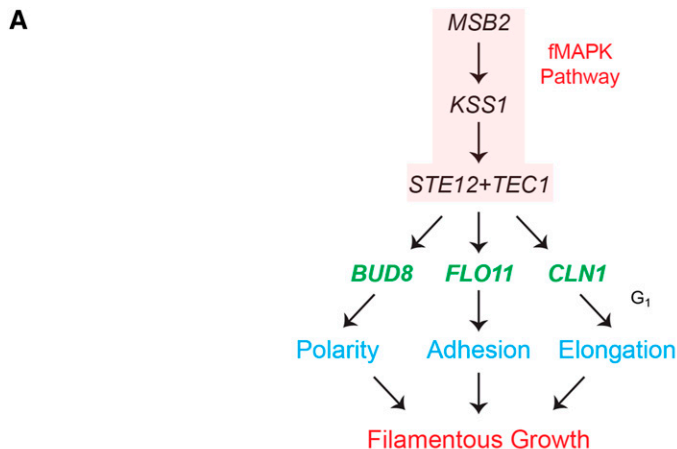
Transcriptional targets of the fMAPK pathway have been identified by comparative expression profiling (Madhani *et al.* 1999; Roberts *et al.* 2000; Heise *et al.* 2010; Adhikari and Cullen 2014; van der Felden *et al.* 2014; Chow *et al.* 2019b). In Adhikari *et al.* (2014), wild-type cells and a fMAPK pathway mutant (*ste12Δ*) were compared in liquid YP-GAL (2% galactose) medium. YP-GAL (2%) medium is an fMAPK pathway-inducing condition that triggers the filamentous growth response (Karunanithi and Cullen 2012; Basu *et al.* 2020). The targets of the pathway identified in Adhikari *et al.* (2014) are shown here in a volcano plot cropped to display only induced targets (Figure 1B). Some highly induced genes are known targets of the pathway (Figure 1, A and B, blue circles, *FLO11* near the center of figure, *CLN1* right side of figure, *BUD8* right side of figure). Other well-characterized targets included *SUC2* (Figure 1B, blue circle near center of figure), which encodes the invertase responsible for hydrolyzing sucrose (Carlson *et al.* 1981) that contributes to social behaviors (Greig and Travisano 2004; Craig Maclean and Brandon 2008; Koschwanez *et al.* 2011) like the formation of invasive aggregates (Chow *et al.* 2019a); the fMAPK pathway components, *MSB2* [mucin sensor, (Cullen *et al.* 2004; Vadaie *et al.* 2008; Pitoniak *et al.* 2009)], *KSS1* [MAP kinase, (Courchesne *et al.* 1989; Roberts and Fink 1994; Bardwell *et al.* 1998a)], *STE12* and *TEC1* (Laloux *et al.* 1990; Chou *et al.* 2006) are induced by the fMAPK pathway to generate positive feedback (Figure 1,

A and B, blue circles). *PGU1* encodes a pectinase (endopolygalacturonase) that does not affect filamentous growth but breaks down plant tissue and may impact nutrient scavenging in the wild (Madhani *et al.* 1999) (Figure 1B, black circle in center of figure). Several mating pathway targets were also identified that are under the control of *Ste12p* (Figure 1, *BAR1*, *STE2*, and *STE4*, black circles); however, the mating pathway is not thought to be required for filamentous growth (Roberts and Fink 1994; Sabbagh *et al.* 2001; Flatauer *et al.* 2005; Meem and Cullen 2012).

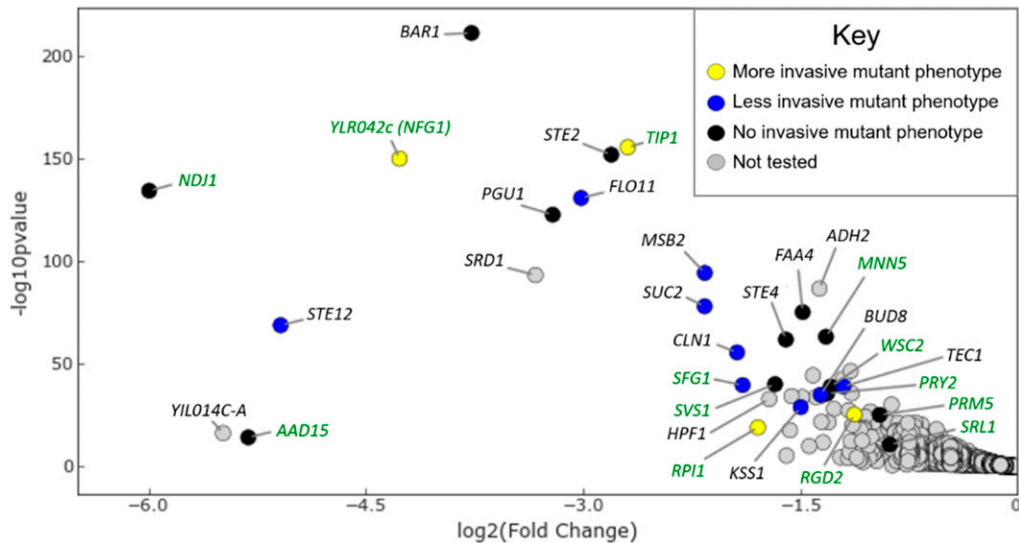
The fMAPK pathway also regulates the expression of targets whose functions remain uncharacterized. Thirteen new transcriptional targets were investigated (Figure 1B, green text, Figure S1) based on their fold change in expression as $\text{Log}_2\text{FoldChange} > |0.8|$. Gene disruptions were constructed in wild-type cells of the filamentous (Σ1278b) background, and deletion mutants were examined for a role in invasive growth. The plate-washing assay was used, where colonies washed off of a surface leave a visible invasive scar (Roberts and Fink 1994). We compared invasive scars of wild-type cells to mutants, looking for an invasive growth phenotype. Because invasive growth occurs in response to limiting carbon (Cullen and Sprague 2000, 2012) and nitrogen (Gimeno *et al.* 1992) and can be induced by high cell density through alcohols (Chen and Fink 2006; González *et al.* 2017; Lenhart *et al.* 2019), the plate-washing assay was performed on different media: YPD (2% Glu), YPD (10% Glu), YPD (16% Glu), YPD high osmolarity medium (2% Glu + 8% Sorbitol), SLAD (low nitrogen), SLAD + 2% ethanol, synthetic dextrose (SD), and YP-GAL (2%).

Most mutants tested did not show a dramatic phenotype in invasive growth (Figure S1). Four mutants (*ylr042cΔ*, *rgd2Δ*, *rpi1Δ*, and *tip1Δ*, Figure 1B, yellow circles) did not show a phenotype on YPD (2% Glu), but showed increased invasive growth on YPD (10% Glu) (see below). This indicates unexpectedly that several highly induced targets of the fMAPK pathway function to negatively regulate invasive growth. Based on data shown below, *YLR042c* was named *NFG1* for Negative Regulator of the Filamentous Growth MAPK pathway 1. Among many mutants tested, one showed a clear invasive growth defect (*sfg1Δ*, Figure 1B, blue circle with green text, and Figure S1) and was also characterized in the study. Five target genes have paralogs that might mask their mutant phenotypes due to genetic redundancy or buffering (Wolfe and Shields 1997; Costanzo *et al.* 2010). Gene disruptions generating *prm5Δ* *ynl058cΔ*, *svs1Δ* *srl1Δ*, and *wsc2Δ* *wsc3Δ* double mutants did not show an invasive growth phenotype (Figure S1). Gene disruptions for *RIB4*, *SRD1*, *HPF1*, *ADA2*, *AAD3* (paralog to *AAD15*), and *PRY1* (paralog to *PRY2*) failed to obtain positive isolates. A genome-wide deletion collection in the Σ1278b background did not contain deletion mutants of *SRD1*, *AAD2*, *RIB4*, *HPF1*, and *AAD15* (Ryan *et al.* 2012), but did for *ADA2*, *PRY1*, and *PRY2*, which did not show an invasive growth phenotype (Ryan *et al.* 2012; Chavel *et al.* 2014). We were successful at assigning roles based on phenotype to 5 of 13 (38%) of the target genes tested. However,

523
524
525
526
527
528
529
530
531
532
533
534
535
536
537
538
539
540
541
542
543
544
545
546
547
548
549
550
551
552
553
554
555
556
557
558
559
560
561
562
563
564
565
566
567
568
569
570
571
572
573
574
575
576
577
578



B *ste12Δ*



62% of the genes failed to produce a phenotype. It is plausible that these genes function in aspects of filamentous growth that are unrelated to agar invasion [for example, *Pgu1p* (Madhani *et al.* 1999)]. Genes that showed a phenotype in invasive growth were verified as targets of the fMAPK pathway by examining their expression by RT-qPCR analysis under conditions that promote filamentous growth (Figure S2, YP-GAL medium). *NFG1*, *RGD2*, *RPI1*, *TIP1*, and *SFG1* may be direct targets because the transcription factors *Ste12p* and *Tec1p* bind to their promoters based on the repository YEASTRACT [<http://www.yeaststract.com/index.php>, (Zeilinger *et al.* 2003; Harbison *et al.* 2004; Borneman *et al.* 2007; Lefrançois *et al.* 2009; Zheng *et al.* 2010)]. Thus, four negative regulators of invasive growth (*NFG1*, *RGD2*, *RPI1*, and *TIP1*) and one positive regulator of invasive growth (*SFG1*) were identified here as fMAPK pathway targets.

Figure 1 Phenotypic analysis for invasive growth of transcriptional targets of the fMAPK pathway identified by comparative RNAseq analysis. (A) A model for the MAPK pathway that regulates filamentous growth by inducing target genes (green) that promote cell adhesion (*FLO11*), cell elongation at G₁ (*CLN1*), and distal-pole budding (*BUD8*). Pathway components are highlighted in red (*MSB2*, *KSS1*, *STE12*, *TEC1*). Not all pathway components are shown. (B) Portion of a volcano plot showing RNAseq data from a previous study (Adhikari and Cullen 2014). x-axis, log₂(FC); y-axis, -log₁₀(P-value). Fold change in gene expression between *ste12Δ* and wild-type cells grown in YP-Gal (2%) for 5.5 hr. All genes labeled have |log₂(FC)| > 0.85 and P-value < 2.5 × 10⁻¹¹. Transposable elements and dubious open reading frames not shown in graph. Green text, genes tested in the study. Yellow, more invasive mutant phenotype. Blue, less invasive mutant phenotype. Black, no invasive mutant phenotype. Gray, not tested.

The fMAPK pathway induces target genes that negatively regulate invasive growth

A major function of the fMAPK pathway is to positively regulate invasive growth [Figure S1, *ste12Δ* (Roberts and Fink 1994; Cook *et al.* 1997; Roberts *et al.* 2000)]. On YPD (10% Glu) medium, the *nfg1Δ*, *rgd2Δ*, *rpi1Δ*, and *tip1Δ* mutants showed increased invasive growth compared to wild type (Figure 2A, Washed), which was confirmed by quantification by ImageJ (Figure 2A, Invasion). Thus, *Nfg1p*, *Rgd2p*, *Rpi1p*, and *Tip1p* have a negative effect on invasive growth. *NFG1* is a highly induced ORF by the fMAPK pathway that has been established as a target for some time with no described function in invasive growth [*YLR042c*, (Caro *et al.* 1997; Hamada *et al.* 1999; Madhani *et al.* 1999; Roberts *et al.* 2000; Giaever *et al.* 2002; Hohmann 2002; García *et al.* 2004; Kim and Levin 2010; Parachin *et al.* 2010; Adhikari and Cullen 2014; Chow *et al.* 2019b)]. *TIP1* encodes a

579
580
581
582
583
584
585
586
587
588
589
590
591
592
593
594
595
596
597
598
599
600
601
602
603
604
605
606
607
608
609
610
611
612
613
614
615
616
617
618
619
620
621
622
623
624
625
626
627
628
629
630
631
632
633
634

635
636 **Table 1 Yeast strains used in this study**
637

Strain	Description	Reference	691
538	MATA SY3089 ste4 FUS1-lacZ FUS1-HIS3 ura3-52	Cullen et al. (2004)	692
539	MATA SY3089 ste4 FUS1-lacZ FUS1-HIS3 ura3-52 ste12::URA3	Pitonik et al. (2009)	693
611	MATA SY3089 ste4 FUS1-lacZ FUS1-HIS3 ura3-52 ste11::URA3	Cullen and Sprague (2002)	694
1029	MATA SY3089 ste4 FUS1-lacZ FUS1-HIS3 ura3-52 flo11::KanMX6	Karunanithi et al. (2010)	695
2043	MATA SY3089 ste4 FUS1-lacZ FUS1-HIS3 ura3-52 FLO11-HA at 1000aa	Karunanithi et al. (2010)	696
2712	MATA SY3089 ste4 FUS1-lacZ FUS1-HIS3 ura3-52 GAL-FLO11	Karunanithi et al. (2010)	697
3039	MATA SY3089 ste4 FUS1-lacZ FUS1-HIS3 ura3-52 Msb2-HA at 500aa DIG1::KIURA3	Chavel et al. (2010)	698
7144	MATA SY3089 ste4 FUS1-lacZ FUS1-HIS3 ura3-52 sfg1::KIURA3	This study	699
7145	MATA SY3089 ste4 FUS1-lacZ FUS1-HIS3 ura3-52 rpi1::KIURA3	This study	700
7146	MATA SY3089 ste4 FUS1-lacZ FUS1-HIS3 ura3-52 rgd2::KIURA3	This study	701
7147	MATA SY3089 ste4 FUS1-lacZ FUS1-HIS3 ura3-52 nfg1::KIURA3	This study	702
7164	MATA SY3089 ste4 FUS1-lacZ FUS1-HIS3 ura3-52 dse1::KIURA3	This study	703
7165	MATA SY3089 ste4 FUS1-lacZ FUS1-HIS3 ura3-52 dse2::KIURA3	This study	704
7166	MATA SY3089 ste4 FUS1-lacZ FUS1-HIS3 ura3-52 dse4::KIURA3	This study	705
7167	MATA SY3089 ste4 FUS1-lacZ FUS1-HIS3 ura3-52 sv1::KIURA3	This study	706
7168	MATA SY3089 ste4 FUS1-lacZ FUS1-HIS3 ura3-52 ndj1::KIURA3	This study	707
7169	MATA SY3089 ste4 FUS1-lacZ FUS1-HIS3 ura3-52 prm5::KIURA3	This study	708
7170	MATA SY3089 ste4 FUS1-lacZ FUS1-HIS3 ura3-52 wsc2::KIURA3	This study	709
7198	MATA SY3089 ste4 FUS1-lacZ FUS1-HIS3 ura3-52 scw11::KIURA3	This study	710
7200	MATA SY3089 ste4 FUS1-lacZ FUS1-HIS3 ura3-52 wsc3::NAT	This study	711
7201	MATA SY3089 ste4 FUS1-lacZ FUS1-HIS3 ura3-52 ynl058c::NAT	This study	712
7202	MATA SY3089 ste4 FUS1-lacZ FUS1-HIS3 ura3-52 svs1::KIURA3 sr1::NAT	This study	713
7203	MATA SY3089 ste4 FUS1-lacZ FUS1-HIS3 ura3-52 prm5::KIURA3 ynl058c::NAT	This study	714
7238	MATA SY3089 ste4 FUS1-lacZ FUS1-HIS3 ura3-52 aad15::KIURA3	This study	715
7239	MATA SY3089 ste4 FUS1-lacZ FUS1-HIS3 ura3-52 hug1::KIURA3	This study	716
7240	MATA SY3089 ste4 FUS1-lacZ FUS1-HIS3 ura3-52 pyr2::KIURA3	This study	717
7241	MATA SY3089 ste4 FUS1-lacZ FUS1-HIS3 ura3-52 mnn5::KIURA3	This study	718
7243	MATA SY3089 ste4 FUS1-lacZ FUS1-HIS3 ura3-52 wsc2::KIURA3 wsc3::NAT	This study	719
7277	MATA SY3089 ste4 FUS1-lacZ FUS1-HIS3 ura3-52 tip1::KIURA3	This study	720
7280	MATA SY3089 ste4 FUS1-lacZ FUS1-HIS3 ura3-52 flo11::Km sfg1::-KIURA3	This study	721
7281	MATA SY3089 ste4 FUS1-lacZ FUS1-HIS3 ura3-52 GAL-FLO11 sfg1::KIURA3	This study	722
7306	MATA SY3089 ste4 FUS1-lacZ FUS1-HIS3 ura3-52 rho5::NAT	This study	723
7321	MATA SY3089 ste4 FUS1-lacZ FUS1-HIS3 ura3-52 FLO11-HA at 1000aa sfg1::KIURA3	This study	724
7536	MATA SY3089 ste4 FUS1-lacZ FUS1-HIS3 ura3-52 nfg1::KIURA3 tip1::NAT	This study	725
7556	MATA SY3089 ste4 FUS1-lacZ FUS1-HIS3 ura3-52 nfg1::KIURA3 tip1::NAT rgd2::KanMX6	This study	726
7557	MATA SY3089 ste4 FUS1-lacZ FUS1-HIS3 ura3-52 nfg1::KIURA3 tip1::NAT rgd2::KanMX6 rpi1::HYG	This study	727

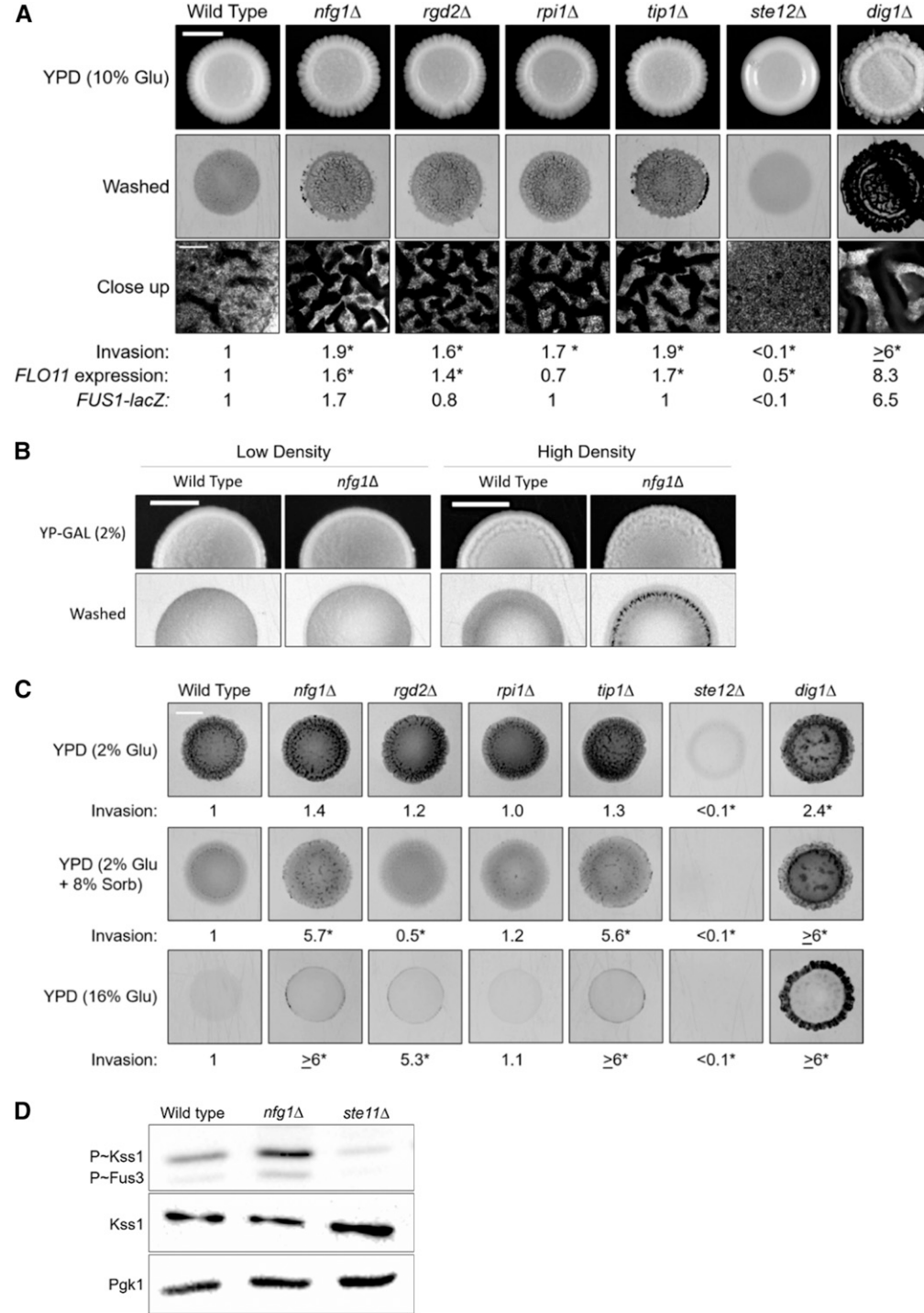
mannoprotein of the fungal cell wall (Kondo and Inouye 1991; Fujii et al. 1999; Chow et al. 2018) and *RGD2* encodes a GTPase-activating protein (RhoGAP for *Cdc42p* and *Rho5p*; Roumanie et al. 2001; Tkach et al. 2012), both with no established role in invasive growth. *RPI1* encodes a transcription factor that inhibits the Ras/cyclic AMP pathway (Kim and Powers 1991), promotes preparation of cells for the stationary phase in part by fortification of the cell wall (Sobering et al. 2002), and increases stress tolerance during fermentation (Puria et al. 2009). *RPI1* was previously shown to

promote filamentous growth in some strain backgrounds but not in the $\sum 1278b$ strain background (Chin et al. 2012).

When compared to the *dig1Δ* mutant, which lacks a known negative regulator of the fMAPK pathway (Cook et al. 1996; Tedford et al. 1997; Bardwell et al. 1998b; Olson et al. 2000), the *nfg1Δ*, *rgd2Δ*, *rpi1Δ*, and *tip1Δ* mutants had more subtle phenotypes (Figure 2A). This suggests Nfg1p, Rgd2p, Rpi1p, and Tip1p might not turn off invasive growth like Dig1p, but instead modulate it in a specific context. One way the fMAPK pathway regulates invasive growth is by regulating the expression of *FLO11*, which encodes the cells' major adhesion

803
 804
 805
 806
 807
 808
 809
 810
 811
 812
 813
 814
 815
 816
 817
 818
 819
 820
 821
 822
 823
 824
 825
 826
 827
 828
 829
 830
 831
 832
 833
 834
 835
 836
 837
 838
 839
 840
 841
 842
 843
 844
 845
 846
 847
 848
 849
 850
 851
 852
 853
 854
 855
 856
 857
 858

Figure 2 Four targets of the fMAPK pathway negatively regulate invasive growth. (A) Plate-washing assay. Wild-type (PC538+pRS316) and the *nfg1Δ* (PC7147), *rgd2Δ* (PC7146), *rpi1Δ* (PC7145), *tip1Δ* (PC7277), *ste12Δ* (PC539), and *dig1Δ* (PC3039) mutants were spotted on YPD (10% Glu) for 3 days. Top row, colonies, middle row, inverted images of plates after wash, Bar, 0.5 cm. Bottom row, close-up of washed plates showing aggregates at 5× magnification, Bar, 400 μm. Invasion, quantification of invasive scars by ImageJ in triplicate, with wild-type values set to 1. Error represents the SEM, which varied <20% across trials. Asterisks, *P*-value <0.035, by Student's *t*-test compared to wild type. *FLO11* expression, fold change in *FLO11* mRNA levels by RT qPCR analysis normalized to *ACT1*. Wild-type value set to 1. Variance by SD was <20% across three trials for all strains, except the *dig1Δ* mutant, which was one trial. Asterisks, *P*-value ≤0.01, by Student's *t*-test compared to wild type. *FUS1-lacZ*, β-Galactosidase (*lacZ*) assays. Cells grown in SD-URA for 16 hr, washed, and resuspended in SGAL-URA for 4.5 hr prior to harvesting cells by centrifugation. (B) Plate-washing assay for wild-type cells (PC538+pRS316) and the *nfg1Δ* mutant (PC7147) grown on YP-Gal (2%) medium. Top row, colonies, bottom row, inverted images of plates after wash, Bar, 0.5 cm. Low Density, cells spotted with OD₆₀₀ = 1.5 for 3 d. High Density, cells spotted with OD₆₀₀ = 11 for 2 days. (C) Plate-washing assay on YPD (2% Glu), high osmolarity medium [YPD (2% Glu + 8% Sorb)], and YPD (16% Glu) for 3 day. Inverted images of plates after wash for indicated strains, Bar, 0.5 cm. Colonies (not shown) were similar in size and appearance. Invasion, quantification of invasive scars by ImageJ in triplicate, with wild type values set to 1. Error represents the SEM, which varied <30% across trials, except the *rpi1Δ* mutant on YPD (16% Glu) varied by <75%. Asterisks, *P*-value < 0.05, by Student's *t*-test compared to wild type. (D) Immunoblot analysis of wild type cells (PC538+pRS316) and the *nfg1Δ* (PC7147) and *ste11Δ* (PC611) mutants grown in SD-URA for 5.5 hr. Cell extracts were probed with antibodies to detect phosphorylated *Kss1p* (P~*Kss1p*) [α -p42/p44], total *Kss1p*, and *Pgk1p* as a control for protein levels. Numbers refer to the ratio of P~*Kss1p* to *Pgk1p* with wild type set to 1. The MAP kinase for the mating pathway, *Fus3p*, also showed some elevated phosphorylation, as might be expected based on a previous report (Basu et al. 2016).



cation of invasive scars by ImageJ in triplicate, with wild type values set to 1. Error represents the SEM, which varied <30% across trials, except the *rpi1Δ* mutant on YPD (16% Glu) varied by <75%. Asterisks, *P*-value < 0.05, by Student's *t*-test compared to wild type. (D) Immunoblot analysis of wild type cells (PC538+pRS316) and the *nfg1Δ* (PC7147) and *ste11Δ* (PC611) mutants grown in SD-URA for 5.5 hr. Cell extracts were probed with antibodies to detect phosphorylated *Kss1p* (P~*Kss1p*) [α -p42/p44], total *Kss1p*, and *Pgk1p* as a control for protein levels. Numbers refer to the ratio of P~*Kss1p* to *Pgk1p* with wild type set to 1. The MAP kinase for the mating pathway, *Fus3p*, also showed some elevated phosphorylation, as might be expected based on a previous report (Basu et al. 2016).

molecule (Lo and Dranginis 1996; Madhani *et al.* 1999; Rupp *et al.* 1999; Roberts *et al.* 2000; Halme *et al.* 2004; Borneman *et al.* 2006; Veelders *et al.* 2010; Adhikari and Cullen 2014; Kraushaar *et al.* 2015; Barua *et al.* 2016; Reynolds 2018; Chow *et al.* 2019b; Brückner *et al.* 2020). RT-qPCR analysis showed that the expression of *FLO11* was elevated in the *nfg1Δ*, *rgd2Δ*, and *tip1Δ* mutants compared to wild type, indicating these genes have an inhibitory effect on *FLO11* expression (Figure 2A, *FLO11* expression). The effect was modest (~0.5-fold), which supports the idea that these genes may be involved in fine tuning invasive growth. As in previous findings (Chin *et al.* 2012), the *rip1Δ* mutant showed no change in the expression of *FLO11* compared to wild type (Figure 2A, *FLO11* expression).

Closer inspection of the invasive scars showed an increase in aggregate invasive growth (Figure 2A, Close up), which results from the interaction of groups of cells that make gouges in the agar (Chow *et al.* 2019a). Likewise, the *nfg1Δ*, *rgd2Δ*, *rip1Δ*, and *tip1Δ* mutants showed elevated aggregate invasive growth on YP-GAL (2%) medium; however, this occurred only when cells were spotted at high cell density (Figure 2B, the complete data set is in Figure S3), which stimulates aggregate invasive growth due to an increased abundance of quorum-sensing molecules (Chow *et al.* 2019a). At standard glucose concentrations [YPD (2% Glu) medium], the *rgd2Δ*, *rip1Δ*, and *tip1Δ* mutants were not more invasive than wild type, and *nfg1Δ* was only slightly more invasive at a *P*-value < 0.062 [Figure 2C, YPD (2% Glu)]. These results indicate Nfg1p, Rgd2p, Rpi1p, and Tip1p inhibit invasive growth more noticeably at higher glucose levels. This observation was puzzling because glucose inhibits invasive growth (Cullen and Sprague 2000). One possibility is that high glucose levels might lead to higher cell density as a result of an elevated carrying capacity (Spor *et al.* 2008). High carrying capacity may lead to enhanced density-dependent invasion after depletion of glucose. Thus, the Nfg1p, Rgd2p, Rpi1p, and Tip1p proteins negatively regulate aggregate invasive growth.

Nfg1p, Rgd2p, Rpi1p, and Tip1p might act separately or in the same pathway. To address this question, the *nfg1Δ*, *rgd2Δ*, *rip1Δ*, and *tip1Δ* mutants were compared by different assays and in different conditions to see if they share the same phenotype. Sharing the same phenotype would suggest that the proteins act in the same pathway. The *nfg1Δ* and *tip1Δ* mutants were phenotypically similar, showing increased invasive growth on different types of media: YPD (10% Glu) [Figure 2A, invasion], YP-GAL (2%) (Figure S3B), high osmolarity medium [YPD (2% Glu + 8% Sorb), Figure 2C], and YPD (16% Glu) (Figure 2C). The *nfg1Δ* and *tip1Δ* mutants also showed the same pattern of *FLO11* expression (Figure 2A, *FLO11* expression). These results support the idea that Nfg1p and Tip1p act in the same pathway.

The *rgd2Δ* and *rip1Δ* mutants were phenotypically similar to the *nfg1Δ* and *tip1Δ* mutants on some media, showing increased invasive growth on YPD (10% Glu) [Figure 2A, invasion] and YP-GAL (2%) (Figure S3B). However, the

rgd2Δ and *rip1Δ* mutants were phenotypically different from the *nfg1Δ* and *tip1Δ* mutants because they did not show increased invasive growth on high osmolarity medium [YPD (2% Glu + 8% Sorb), Figure 2C]. The *rgd2Δ* and *rip1Δ* mutants were also phenotypically different from each other on high osmolarity medium [YPD (2% Glu + 8% Sorb), Figure 2C] and YPD (16% Glu) (Figure 2C). Furthermore, Rgd2p but not Rpi1p regulated *FLO11* expression (Figure 2A, *FLO11* expression). Overall, these results suggest Rgd2p and Rpi1p function in different pathways.

Mutant combinations were generated (*nfg1Δ tip1Δ* double mutant, *nfg1Δ tip1Δ rgd2Δ* triple mutant, and *nfg1Δ tip1Δ rgd2Δ rip1Δ* quadruple mutant) to determine if they had additive phenotypes. Additive phenotypes would suggest the proteins operate in different pathways. The *nfg1Δ* single mutant, the *nfg1Δ tip1Δ* double mutant, the *nfg1Δ tip1Δ rgd2Δ* triple mutant, and the *nfg1Δ tip1Δ rgd2Δ rip1Δ* quadruple mutant showed increased invasive growth compared to wild type but did not show strong phenotypic differences from each other by the plate-washing assay (Figure S4, A and B). Collectively, evidence from the plate-washing assay of single mutants and combination mutants suggests Rgd2p and Rpi1p function separately from each other and from Nfg1p and Tip1p, while Nfg1p and Tip1p may act in the same pathway.

The fMAPK pathway is one of the pathways that regulates *FLO11* expression (Madhani *et al.* 1999; Rupp *et al.* 1999; Borneman *et al.* 2006; Chavel *et al.* 2010, 2014; Cullen and Sprague 2012). Given that Nfg1p, Rgd2p, and Tip1p have a negative effect on *FLO11* expression, they might do so by dampening the fMAPK pathway. The *nfg1Δ* mutant, but not the *tip1Δ*, *rgd2Δ*, or *rip1Δ* mutant showed elevated fMAPK pathway activity based on a transcriptional reporter [Figure 2A, *FUS1-lacZ*]. This indicates that Nfg1p negatively regulates the fMAPK pathway. Double, triple, and quadruple mutant analysis showed that the *nfg1Δ tip1Δ* double mutant had an additional increase in fMAPK pathway activity compared to the *nfg1Δ* single mutant (Figure S4A, *FUS1-lacZ*). Thus, Tip1p might also negatively regulate the fMAPK pathway under some conditions separately from Nfg1p, although we have not explored this possibility. These results indicate Nfg1p and Tip1p act, at least in part, in separate ways. Immunoblot analysis with antibodies that detect phosphorylated (P~) Kss1p (the MAP Kinase of the fMAPK pathway) showed that P~Kss1p levels were higher in the *nfg1Δ* mutant (Figure 2D), compared to wild-type cells and the *ste11Δ* mutant [*Ste11p* is the MAP kinase kinase kinase that phosphorylates the MAP kinase kinase, *Ste7p*, which phosphorylates Kss1p (Liu *et al.* 1993; Roberts and Fink 1994)]. Thus, Nfg1p, Rgd2p, Rpi1p, and Tip1p have separate functions in the negative regulation of invasive growth, and Nfg1p (and perhaps Tip1p) negatively regulates the fMAPK pathway.

We performed comparative assessments of Nfg1p, Rgd2p, Rpi1p, and Tip1p by BLAST. Nfg1p protein sequence had similarity only within the *Saccharomyces* clade, with *Saccharomyces eubayanus* being the most distant relative

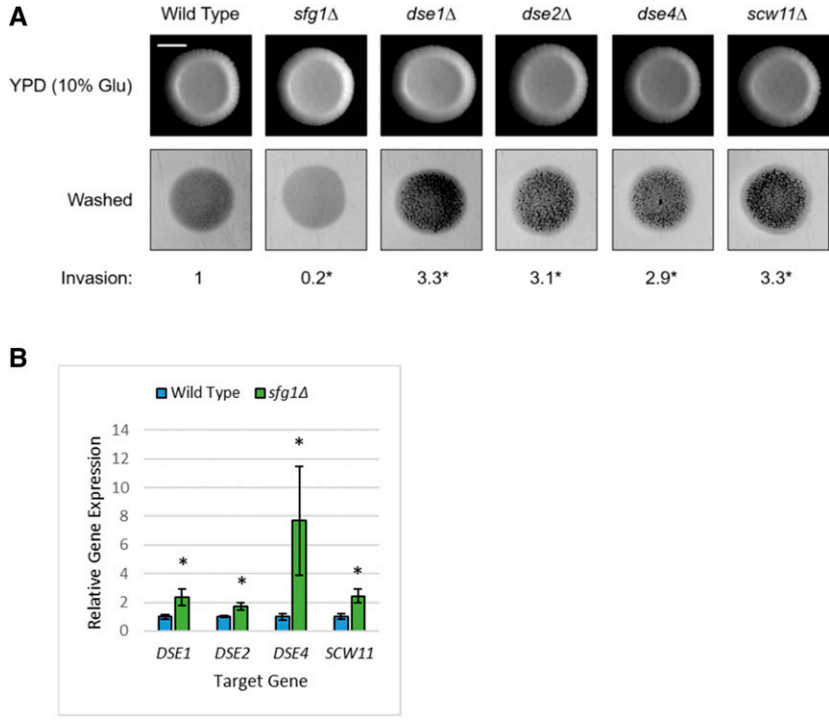


Figure 3 Transcriptional targets of Sfg1p that induce cell separation inhibit invasive growth. (A) Plate-wash assay for wild-type cells (PC538+pRS316) and the *sfg1Δ* (PC7144), *dse1Δ* (PC7164), *dse2Δ* (PC7165), *dse4Δ* (PC7166), and *scw11Δ* (PC7198) mutants spotted onto YPD (10% Glu) for 3 days. Top row, colonies, bottom row, inverted images of invasive scar after plate wash, Bar, 0.5 cm. Invasion, quantification of invasive scars by ImageJ in triplicate, with wild-type values set to 1. Error represents the SEM, which varied <45% across trials, except the *sfg1Δ* mutant which varied by <56%. Asterisks, *P*-value <0.035, by Student's *t*-test compared to wild type. (B) Relative gene expression by RT-qPCR of target gene (*DSE1*, *DSE2*, *DSE4*, and *SCW11*) mRNA levels, normalized to *ACT1* expression, between wild-type (PC538) and *sfg1Δ* (PC7144) cells grown in YP-Gal (2%) liquid medium for 32 hr. Wild-type values set to 1. Error represents SD across three trials. Asterisks, *P*-value < 0.02, by Student's *t*-test compared to wild type.

with a recognizable homolog (Figure S5, A and B); therefore, **Nfg1p** is not a conserved protein that regulates the fMAPK pathway across all yeasts. The protein sequences of **Rgd2p**, **Rpi1p**, and **Tip1p** had homologs in other yeasts outside the *Saccharomyces* clade (Figure S5, A and B), including *Candida glabrata*—a human pathogen that undergoes filamentous growth (Fidel *et al.* 1999; Csank and Haynes 2000; Rodrigues *et al.* 2014). **Rgd2p** also had protein sequence similarity to a homolog in the human pathogen *C. albicans* (Figure S5, A and B). Thus, **Rgd2p**, **Rpi1p**, and **Tip1p** are conserved in several yeast species and could be regulators of filamentous growth in pathogenic yeasts.

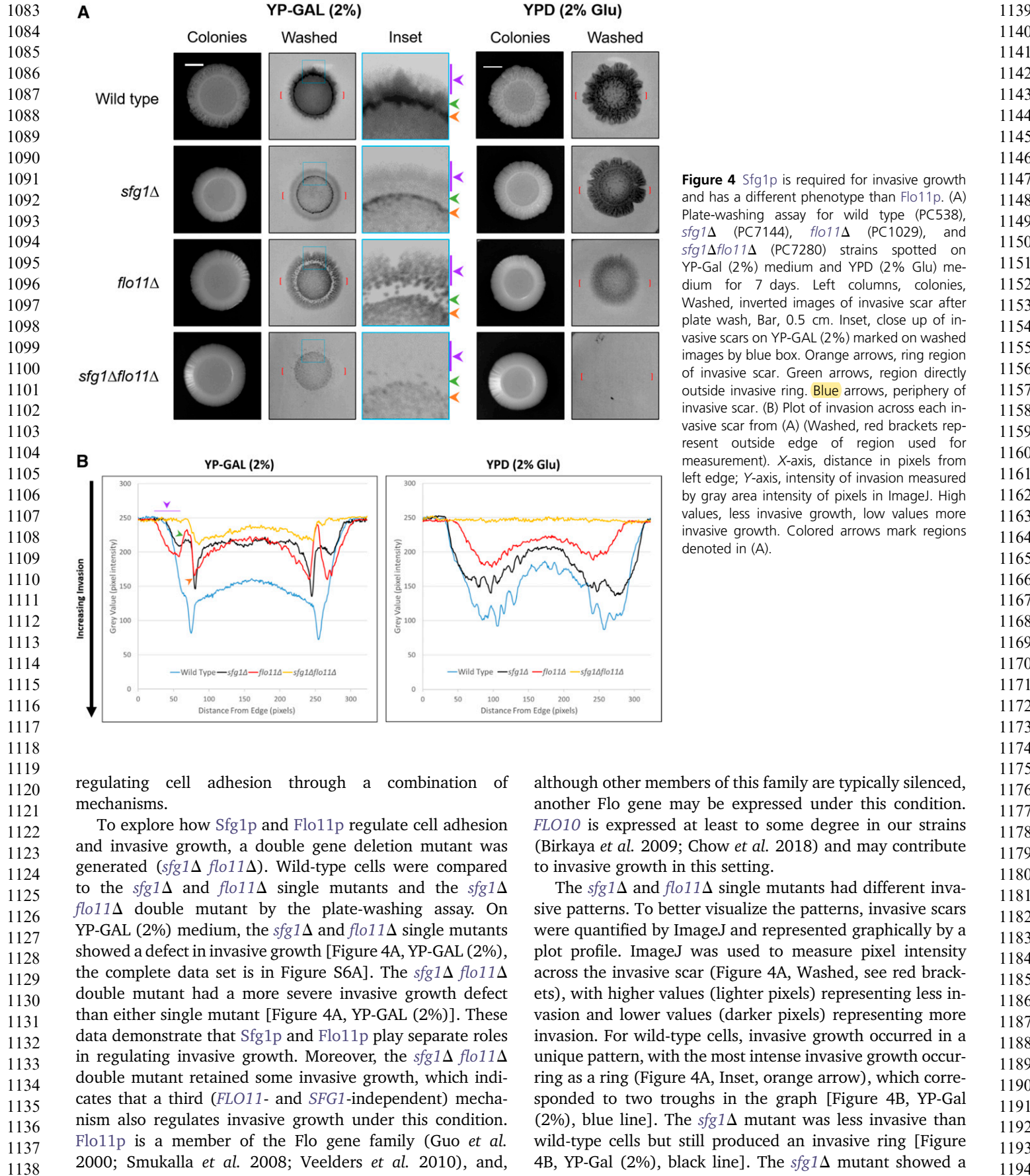
Sfg1p negatively regulates the transcription of cell separation genes

Sfg1 was identified as a target of the fMAPK pathway (Figure 1B, blue circle with green text) and positive regulator of invasive growth (Figure S1, Third column). *Sfg1p* is a transcription factor that induces superficial pseudohyphal growth [a type of growth where cells spread across a surface in filament-like structures (Fujita *et al.* 2005)] and transcriptionally represses genes that induce cell separation, including *DSE1*, *DSE2*, *DSE4*, and *SCW11* (Doolin *et al.* 2001; Baladrón *et al.* 2002; Draper *et al.* 2009; White *et al.* 2009). The inhibition of cell separation leads to filament formation (King and Butler 1998; Doolin *et al.* 2001). *DSE2*, *DSE4*, and *SCW11* have similarity to glucanases and may promote cell separation by degrading the cell wall between mother and daughter cells. To determine whether *Sfg1p* regulates invasive growth by this mechanism, the transcriptional targets of *Sfg1p* that induce cell separation were tested for a role in

invasive growth. Wild-type cells and the *sfg1Δ*, *dse1Δ*, *dse2Δ*, *dse4Δ* and *scw11Δ* mutants were examined for invasive growth by the plate-washing assay (Figure 3A). The *dse1Δ*, *dse2Δ*, *dse4Δ* and *scw11Δ* mutants had increased invasive growth compared to wild-type cells, supporting the idea that these genes have an inhibitory effect on invasive growth. *DSE1*, *DSE2*, *DSE4* and *SCW11* were transcriptional targets of *Sfg1p* by RT-qPCR analysis being upregulated in the *sfg1Δ* mutant under conditions that promote filamentous growth (Figure 3B, YP-GAL medium). Thus, in support of previous findings, *Sfg1p* inhibits the transcription of genes that promote cell separation, which results in increased cell attachment and invasive growth.

SFG1* regulates invasive growth independently from *FLO11

One requirement for invasive growth is cell adhesion by *Flo11p* (Lo and Dranginis 1996; Madhani *et al.* 1999; Rupp *et al.* 1999; Halme *et al.* 2004; Borneman *et al.* 2006; Veelders *et al.* 2010; Kraushaar *et al.* 2015; Barua *et al.* 2016; Reynolds 2018). *Flo11p* binds in a homotypic manner to other *Flo11p* molecules to maintain adhesive contacts between cells (Kraushaar *et al.* 2015; Brückner *et al.* 2020). The expression of *FLO11* is regulated by the fMAPK pathway (Madhani *et al.* 1999; Rupp *et al.* 1999; Roberts *et al.* 2000; Borneman *et al.* 2006; Adhikari and Cullen 2014; Chow *et al.* 2019b). Presumably, *Sfg1p* (by inhibiting cell separation) and *Flo11p* (by promoting homotypic contacts) function in different ways to control filamentous growth. The fact that *SFG1* and *FLO11* expression are both regulated by the fMAPK pathway suggests that the pathway may have versatility in



regulating cell adhesion through a combination of mechanisms.

To explore how *Sfg1p* and *Flo11p* regulate cell adhesion and invasive growth, a double gene deletion mutant was generated (*sfg1Δ flo11Δ*). Wild-type cells were compared to the *sfg1Δ* and *flo11Δ* single mutants and the *sfg1Δ flo11Δ* double mutant by the plate-washing assay. On YP-GAL (2%) medium, the *sfg1Δ* and *flo11Δ* single mutants showed a defect in invasive growth [Figure 4A, YP-GAL (2%)], the complete data set is in Figure S6A]. The *sfg1Δ flo11Δ* double mutant had a more severe invasive growth defect than either single mutant [Figure 4A, YP-GAL (2%)]. These data demonstrate that *Sfg1p* and *Flo11p* play separate roles in regulating invasive growth. Moreover, the *sfg1Δ flo11Δ* double mutant retained some invasive growth, which indicates that a third (*FLO11*- and *SFG1*-independent) mechanism also regulates invasive growth under this condition. *Flo11p* is a member of the Flo gene family (Guo *et al.* 2000; Smukalla *et al.* 2008; Veelders *et al.* 2010), and,

although other members of this family are typically silenced, another Flo gene may be expressed under this condition. *FLO10* is expressed at least to some degree in our strains (Birkaya *et al.* 2009; Chow *et al.* 2018) and may contribute to invasive growth in this setting.

The *sfg1Δ* and *flo11Δ* single mutants had different invasive patterns. To better visualize the patterns, invasive scars were quantified by ImageJ and represented graphically by a plot profile. ImageJ was used to measure pixel intensity across the invasive scar (Figure 4A, Washed, see red brackets), with higher values (lighter pixels) representing less invasion and lower values (darker pixels) representing more invasion. For wild-type cells, invasive growth occurred in a unique pattern, with the most intense invasive growth occurring as a ring (Figure 4A, Inset, orange arrow), which corresponded to two troughs in the graph [Figure 4B, YP-Gal (2%), blue line]. The *sfg1Δ* mutant was less invasive than wild-type cells but still produced an invasive ring [Figure 4B, YP-Gal (2%), black line]. The *sfg1Δ* mutant showed a

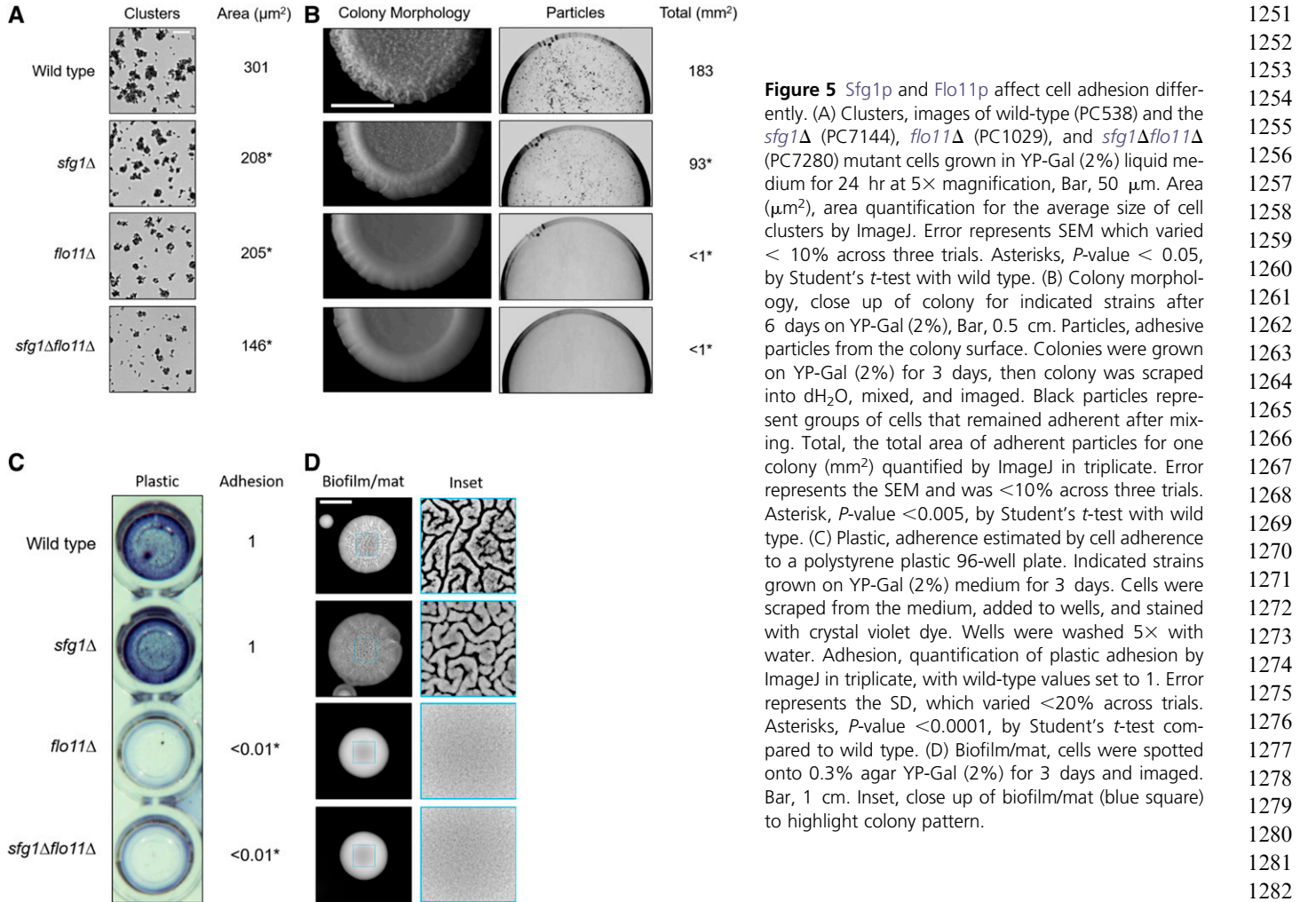


Figure 5 *Sfg1p* and *Flo11p* affect cell adhesion differently. (A) Clusters, images of wild-type (PC538) and the *sfg1 Δ* (PC7144), *flo11 Δ* (PC1029), and *sfg1 Δ flo11 Δ* (PC7280) mutant cells grown in YP-Gal (2%) liquid medium for 24 hr at 5 \times magnification, Bar, 50 μm . Area (μm^2), area quantification for the average size of cell clusters by ImageJ. Error represents SEM which varied < 10% across three trials. Asterisks, P -value < 0.05, by Student's *t*-test with wild type. (B) Colony morphology, close up of colony for indicated strains after 6 days on YP-Gal (2%), Bar, 0.5 cm. Particles, adhesive particles from the colony surface. Colonies were grown on YP-Gal (2%) for 3 days, then colony was scraped into dH₂O, mixed, and imaged. Black particles represent groups of cells that remained adherent after mixing. Total, the total area of adherent particles for one colony (mm^2) quantified by ImageJ in triplicate. Error represents the SEM and was <10% across three trials. Asterisk, P -value <0.005, by Student's *t*-test with wild type. (C) Plastic, adherence estimated by cell adherence to a polystyrene plastic 96-well plate. Indicated strains grown on YP-Gal (2%) medium for 3 days. Cells were scraped from the medium, added to wells, and stained with crystal violet dye. Wells were washed 5 \times with water. Adhesion, quantification of plastic adhesion by ImageJ in triplicate, with wild-type values set to 1. Error represents the SD, which varied <20% across trials. Asterisks, P -value <0.0001, by Student's *t*-test compared to wild type. (D) Biofilm/mat, cells were spotted onto 0.3% agar YP-Gal (2%) for 3 days and imaged. Bar, 1 cm. Inset, close up of biofilm/mat (blue square) to highlight colony pattern.

similar level of invasion as the *flo11 Δ* mutant [Figure 4B, YP-Gal (2%), compare black and red lines] but was more invasive in the ring region (orange arrows) and just outside of the ring region (green arrows) than the *flo11 Δ* mutant. Thus, in these regions *Flo11p* plays a bigger role in invasive growth than *Sfg1p*. Along the periphery of the invasive scar, the *flo11 Δ* mutant was more invasive than the *sfg1 Δ* mutant (Figure 4, A and B, YP-Gal (2%), purple arrows), indicating that in this region, *Sfg1p* plays a bigger role in invasive growth than *Flo11p*. Surprisingly, the *flo11 Δ* mutant was more invasive than wild type at the periphery (purple arrows). Thus, colonies do not invade in an 'all or none' manner. Rather, cells in different parts of the colony show different levels of invasion that are differentially regulated by *Sfg1p* and *Flo11p*.

Many adhesion-dependent responses are regulated by the fMAPK pathway (Chow *et al.* 2019b). For example, cells can form adherent flocs in liquid culture (Verstrepen *et al.* 2003; Halme *et al.* 2004; Fidalgo *et al.* 2006; Barua *et al.* 2016). To examine the role of *Sfg1p* and *Flo11p* in this aspect of cell adhesion, we developed an assay to quantify cell adhesion in

liquid cultures. This was done by measuring the average area of a group (cluster) of adherent cells by ImageJ after growth in liquid YP-GAL (2%) medium for 24 hr. The *flo11 Δ* and *sfg1 Δ* single mutants showed a defect in forming clusters (Figure 5A). The *sfg1 Δ flo11 Δ* double mutant showed a more severe defect. Thus, *Sfg1p* and *Flo11p* contribute equally in regulating cell adhesion in liquid.

Environmental impacts on *Sfg1p*- and *Flo11p*-mediated adhesion

Other adhesion-dependent responses require *Flo11p*, such as complex colony morphology, where patterns/ruffles form on the colony surface (Granek and Magwene 2010; Karunanithi *et al.* 2012; Chow *et al.* 2019b). The *sfg1 Δ* mutant had an intermediate complex colony morphology phenotype between wild-type cells and the *flo11 Δ* mutant (Figure 5B, Colony Morphology). By this criterion, the *sfg1 Δ flo11 Δ* double mutant was indistinguishable from the *flo11 Δ* mutant. To further investigate this cell-adhesion phenotype, we developed an assay to quantify cell adhesion within colonies. Cells were scraped from the surface of colonies grown on semisolid

1307 agar medium, resuspended in dH₂O and mixed. Particles
1308 made up of adherent cells were imaged and quantified as
1309 the area of all particles (total) per colony. Cells derived from
1310 wild-type colonies formed particles that were visible to the
1311 eye, while cells of the *flo11* Δ mutant separated and were not
1312 visible by eye [Figure 5B, Particles and Total]. The *sfg1* Δ
1313 mutant had an intermediate phenotype (Figure 5B, Particles
1314 and Total). The *sfg1* Δ *flo11* Δ double mutant was indistin-
1315 guishable from the *flo11* Δ mutant by this assay. Thus, *Sfg1p*
1316 plays a minor role compared to *Flo11p* in this adhesion-de-
1317 pendent phenotype. This is different from the role of *Sfg1p*
1318 in invasive growth and adhesion in liquid where it played the
1319 same role as *Flo11p*.

1320 Some species of yeast, such as *C. albicans*, are pathogens
1321 whose adhesion-related behaviors promote virulence. For ex-
1322 ample, many species of fungi, including pathogens, form bio-
1323 films or mats (Lo *et al.* 1997; Reynolds and Fink 2001; Kabir
1324 *et al.* 2012; Karunanithi *et al.* 2012; Silva-Dias *et al.* 2015).
1325 Biofilm/mats occur when cells adhere together in a complex
1326 multicellular community (Costerton *et al.* 1999; Reynolds
1327 and Fink 2001; Flemming and Wingender 2010; Kabir *et al.*
1328 2012; Karunanithi *et al.* 2012; Azeredo *et al.* 2017). In this
1329 growth mode, cells can adhere to inert surfaces, like plastics,
1330 which occurs on medical devices and hospital settings
1331 (Kennedy *et al.* 1989; Reynolds and Fink 2001; Kabir *et al.*
1332 2012; Karunanithi *et al.* 2012; Silva-Dias *et al.* 2015). Bio-
1333 film/mat formation and plastic adhesion also occur in *S.
1334 cerevisiae*, and requires *Flo11p* [Figure 5, C and D,
1335 (Reynolds and Fink 2001; Karunanithi *et al.* 2012)]. *Sfg1p*
1336 was not required for plastic adhesion (Figure 5C) or biofilm/
1337 mat expansion and ruffling (Figure 5D). This result indicates
1338 *Sfg1p* is required for a subset of *Flo11p*-dependent cell-ad-
1339 hesion phenotypes. To summarize, depending on the cell-
1340 adhesion phenotype, *Sfg1p* contributes equally to cell adhe-
1341 sion compared to *Flo11p*, contributes less, or does not con-
1342 tribute at all.

1343 We also asked whether the environment might impact the
1344 way that *Sfg1p* and *Flo11p* regulate invasive growth. Com-
1345 pared to YP-GAL (2%), on YPD (2% Glu) medium, the *sfg1* Δ
1346 mutant was only slightly defective for invasive growth,
1347 whereas the *flo11* Δ mutant was more defective [Figure 4A,
1348 YPD (2% Glu), the complete data set is in Figure S6B]. The
1349 difference in invasive growth was also evident in the invasive
1350 patterns. In particular, the *flo11* Δ mutant was less invasive
1351 than the *sfg1* Δ mutant across the entire plot profile [Figure
1352 4B, YPD (2% Glu), compare red and black lines]. The *sfg1* Δ
1353 *flo11* Δ double mutant showed no invasive growth on YPD
1354 (2% Glu) [Figure 4, A and B, compare the yellow lines in
1355 GLU and GAL], indicating that *Sfg1p* and *Flo11p* solely con-
1356 trol invasive growth under this condition. Furthermore,
1357 *Flo11p* showed different requirements in liquid compared
1358 to surface growth. In liquid, the *flo11* Δ mutant had a ~1.5-
1359 fold decrease in adhesion, compared to ~183-fold decrease
1360 on semisolid agar medium (Figure 5A, Area, and Figure 5B,
1361 Total). *Sfg1p* regulated cell adhesion in liquid and on semi-
1362 solid agar media similarly, because the *sfg1* Δ mutant showed

1363 ~twofold decrease under both conditions (Figure 5A, Area,
1364 and Figure 5B, Total). Therefore, *Sfg1p* and *Flo11p* play dif-
1365 ferent roles in adhesion-dependent responses depending on
1366 the environment.

1367 *Sfg1p regulates multiple aspects of filamentous growth*

1368 Biofilm/mats are embedded in a matrix that is synthesized by
1369 the microbial community (Costerton *et al.* 1999; Flemming
1370 and Wingender 2010; Kabir *et al.* 2012; Azeredo *et al.* 2017).
1371 In *S. cerevisiae*, *Flo11p* is shed in biofilms/mats into the ex-
1372 tracellular milieu (Karunanithi *et al.* 2010). Given that *Sfg1p*
1373 impacts the expression of cell wall enzymes, *Sfg1p* was tested
1374 for a role in regulating *Flo11p* shedding. A wild-type
1375 HA-tagged *Flo11p* strain (*FLO11-HA*) and a *sfg1* Δ
1376 *FLO11-HA* mutant were grown on a nitrocellulose membrane
1377 laid on YP-Gal (2%) semisolid medium. The membrane was
1378 washed and probed by antibodies for the HA epitope.
1379 *Flo11p*-HA shedding was reduced in the *sfg1* Δ *FLO11*-HA
1380 mutant compared to the wild-type *FLO11*-HA strain (Figure
1381 6A). Many transcription factors converge on the *FLO11*
1382 promoter (Borneman *et al.* 2006); therefore, *Sfg1p* might impact
1383 *Flo11p* shedding by regulating expression of the *FLO11* gene.
1384 RT-qPCR analysis showed that *FLO11* expression was re-
1385duced in the *sfg1* Δ mutant compared to wild-type cells (Fig-
1386 ure 6A, *FLO11* expression). Therefore, *Sfg1p* regulates cell
1387 adhesion in part by regulating *FLO11* expression. *Sfg1p*
1388 might also impact *Flo11p* shedding through cell wall
1389 remodeling.

1390 To determine the role of *Sfg1p* in regulating cell adhesion
1391 independent of *FLO11* expression, a strain where *FLO11*
1392 is expressed from a galactose-inducible promoter (*GAL-FLO11*)
1393 was compared to the *sfg1* Δ *GAL-FLO11* mutant for invasive
1394 growth and cluster formation. Overexpression of *FLO11*
1395 caused increased invasive growth [Figure 6B, washed,
1396 (Chow *et al.* 2019a)] and the formation of large clusters
1397 (Figure 6B, Clusters and Area). Deletion of *SFG1* in the
1398 *GAL-FLO11* strain led to a decrease in invasive growth and
1399 reduced cluster size (Figure 6B). This data indicates that
1400 *Sfg1p* primarily regulates cell adhesion independent of
1401 *FLO11* expression. As shown above, *Sfg1p* had no effect on
1402 some *Flo11p*-dependent responses, like biofilm/mat forma-
1403 tion and plastic adhesion. Thus, *Sfg1p* might not regulate
1404 *FLO11* expression under all conditions. This idea is supported
1405 by the fact that *Sfg1p* did not regulate *Flo11p* shedding under
1406 all conditions (Figure S7).

1407 In addition to cell adhesion, cells undergoing filamentous
1408 growth also regulate cell elongation. Cells elongate by a delay
1409 in the cell cycle that leads to extended apical growth (Kron
1410 *et al.* 1994; Edgington *et al.* 1999). The fMAPK pathway
1411 causes a delay in the cell cycle by inducing expression of
1412 the *CLN1* gene (Loeb *et al.* 1999; Madhani *et al.* 1999), which
1413 encodes a G₁/S specific cyclin (Hadwiger *et al.* 1989). How-
1414 ever, this is not the only way the fMAPK pathway induces a
1415 delay in the cell cycle (Ahn *et al.* 1999). One additional way
1416 may be through regulating the expression of *SFG1* because
1417 *SFG1* regulates the cell cycle (White *et al.* 2009). A *sfg1* Δ

1419
1420
1421
1422
1423
1424
1425
1426
1427
1428
1429
1430
1431
1432
1433
1434
1435
1436
1437
1438
1439
1440
1441
1442
1443
1444
1445
1446
1447
1448
1449
1450
1451
1452
1453
1454
1455
1456
1457
1458
1459
1460
1461
1462
1463
1464
1465
1466
1467
1468
1469
1470
1471
1472
1473
1474

A

	Flo11-HA		
	Control	Wild Type	<i>sfg1Δ</i>
YP-Gal (2%)			
IB anti-HA			
IB anti-HA:	<0.01*	1	0.3*
<i>FLO11</i> expression:	N/A	1	0.6*

B

	SGAL(2%)	Washed	Clusters	Area (μm^2)
Wild Type				301
<i>GAL-FLO11</i>				628*
<i>sfg1ΔGAL-FLO11</i>				275

C

	Wild Type	<i>sfg1Δ</i>	<i>GAL-SFG1</i>
YP-GAL (2%)			

Figure 6 Sfg1p regulates *FLO11* expression and cell elongation. (A) Colony immunoblot to detect HA-*Flo11p* with anti-HA antibodies. Wild type (PC538), *FLO11*-HA (PC2043), and *sfg1ΔFLO11*-HA (PC7321) strains grown on nitrocellulose membranes atop YP-Gal (2%) semisolid agar medium for 3 days. Numbers refer to the intensity of anti-HA quantified by image lab. Experiments were performed in triplicate. Error is SEM with <20% variation across trials. Asterisks, *P*-value <0.02, by Student's *t*-test compared to wild type. *FLO11* expression, fold change in *FLO11* mRNA levels by RT qPCR analysis normalized to *ACT1*, wild-type values set to 1. *FLO11* expression was measured in wild-type (PC538) and *sfg1Δ* (PC7144) strains. Error represents SD, which varied <30% across trials. Asterisks, *P*-value <0.03, by Student's *t*-test with wild type. (B) Left and middle columns, Plate-washing assay for wild type (PC538), Gal-*FLO11* (PC2712) *sfg1ΔGal-FLO11* (PC7281) strains on SGAL+AA after 6 days. Left column, before wash and middle column, after wash, Bar, 0.5 cm. Right column, images of cells grown in YP-Gal (2%) liquid medium for 24 hr imaged at 5× magnification, Bar, 50 μm. Area values represent ImageJ quantification for the average size of cell clusters by area (μm²) for indicated strains. Error represents SEM which varied <15% across three trials. Asterisk, *P*-value = 0.01, by Student's *t*-test with wild type. Wild-type data are from Figure 3. (C) Cell morphology compared after growth in YP-Gal (2%) for 4 hr between wild type (PC538), *sfg1Δ* (PC7144), and wild type transformed with a plasmid containing an overexpression of *SFG1* by a galactose-inducible promoter (pGAL-SFG1). Bar, 10 μm.

mutant is delayed in the G₁ phase of the cell cycle, and *SFG1* overexpression causes a delay in G₂/M (White *et al.* 2009). We found by microscopy, the *sfg1*Δ mutant had a round-cell morphology compared to wild-type cells, and overexpression of *SFG1* by a galactose-inducible promoter [pGAL-*SFG1* (Gelperin *et al.* 2005)] induced an elongated morphology (Figure 6C). Thus, the fMAPK pathway may regulate cell elongation by multiple mechanisms, such as by controlling the expression of the *CLN1* and *SFG1* genes.

Sfg1p was previously shown to be a distantly related member of a family of transcriptional regulators of fungal development in nonpathogenic and pathogenic fungi because it has weak similarity in protein sequence to a family of transcription factors involved in pseudohyphal/hyphal

development (Fujita *et al.* 2005). These include *Phd1p* and *Sok2p* in *S. cerevisiae* (Gimeno and Fink 1994; Ward *et al.* 1995; Fujita *et al.* 2005); *Efg1p* in *C. albicans* (Stoldt *et al.* 1997; Fujita *et al.* 2005); *StuA* in *Aspergillus nidulans* (Miller *et al.* 1992; Fujita *et al.* 2005); and *Asm-1* in *Neurospora crassa* (Aramayo *et al.* 1996; Fujita *et al.* 2005). We found that *SFG1* shows synteny (by the Yeast Gene Order browser) and protein sequence similarity (by BLAST) to other fungi species as well (Figure S5, A and B), including an uncharacterized ORF (CAGL0I09856g) in the human pathogen *C. glabrata* (Fidel *et al.* 1999; Csank and Haynes 2000; Rodrigues *et al.* 2014). Presumably, *SFG1* is required for filamentous growth in other fungal species besides *S. cerevisiae*,

1531
1532
1533
1534
1535
1536
1537
1538
1539
1540
1541
1542
1543
1544
1545
1546
1547
1548
1549
1550
1551
1552
1553
1554
1555
1556
1557
1558
1559
1560
1561
1562
1563
1564
1565
1566
1567
1568
1569
1570
1571
1572
1573
1574
1575
1576
1577
1578
1579
1580
1581
1582
1583
1584
1585
1586

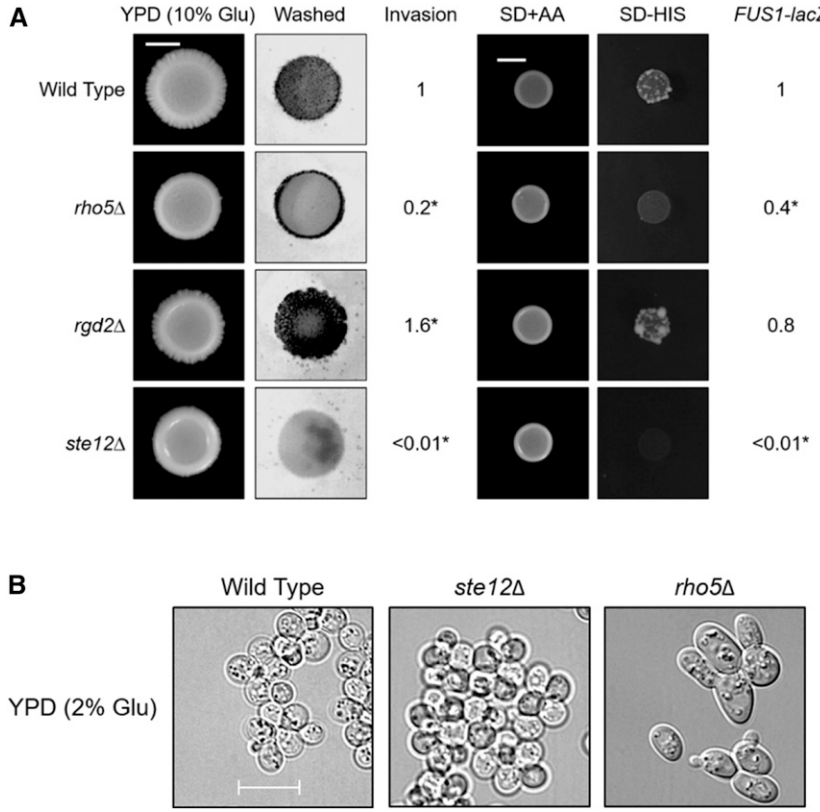


Figure 7 *Rho5p* regulates the fMAPK pathway. (A) Plate-washing assay of wild type (PC538+pRS316) and the *rho5Δ* (PC7306), *rgd2Δ* (PC7146), and *ste12Δ* (PC539) mutants spotted on YPD (10% Glu) and grown for 3 days. Left column, colonies, second column, inverted images of plates after wash, Bar, 0.5 cm. Invasion, quantification of invasive scars by ImageJ in triplicate, with wild type values set to 1. Error represents the SEM, which varied $\leq 50\%$ across three trials. Asterisks, P -value < 0.035 , by Student's *t*-test compared to wild type. The *rgd2Δ* mutant invasion value is from Figure 2. SD+AA, strains spotted onto SD+AA and grown for 3 days. SD-HIS, transcriptional (growth) reporter [*FUS1-HIS3*]. Strains grown on SD-URA for 16 hr, washed, and resuspended in YPD (10% Glu) medium for 6.5 hr prior to harvesting cells by centrifugation. Error represents SEM, which varied $< 10\%$ across three trials. Asterisk, P -value < 0.01 . (B) Cell morphology compared after growth in YPD (2% Glu) for 16 hr between indicated strains. Bar, 10 μ m.

and may be an important regulator in some pathogenic yeasts.

RHO5 regulates the activity of the fMAPK pathway

Rho5p is a small GTPase of the Rho family (Garcia-Ranea and Valencia 1998; Singh *et al.* 2008, 2019; Schmitz *et al.* 2018). *RHO5* was not a target of the fMAPK pathway; however, it is regulated by the GTPase-activating protein *Rgd2p* (Annan *et al.* 2008), which was a target of the fMAPK pathway (Figure 1B). The plate-washing assay showed that the *rho5Δ* mutant was defective for invasive growth (Figure 7A, Washed and Invasion) supporting previous observations (Ryan *et al.* 2012; Foster *et al.* 2013). To explore if *Rho5p* regulates invasive growth through the fMAPK pathway, the *rho5Δ* mutant was tested for fMAPK pathway activity by a transcriptional (growth) reporter [*FUS1-HIS3*] and a *lacZ* reporter [*FUS1-lacZ*]. Both reporters reflect the activity of the fMAPK pathway in cells lacking an intact mating pathway [*ste4Δ* (Cullen *et al.* 2004)]. The *rho5Δ* mutant was defective for fMAPK pathway activity based on growth on SD-HIS media (Figure 7A, SD-HIS). This was not due to a growth defect on synthetic media (Figure 7A, SD+AA). The fMAPK pathway also showed reduced activity in the *rho5Δ* mutant by the *FUS1-lacZ* reporter (Figure 7A, *FUS1-lacZ*). These results indicate that *Rho5p* may play a subtle role in regulating the fMAPK pathway. We did not find a link between *Rgd2p* and *Rho5p* in the regulation of the fMAPK pathway because the *rgd2Δ* mutant, unlike the *rho5Δ* mutant, did not show a

change in fMAPK pathway activity by the *FUS1-HIS3* or the *FUS1-lacZ* reporters (Figure 7A). By microscopy, the *rho5Δ* mutant also showed misshaped cell morphology and improper budding (Figure 7B). Overall, the data establishes *Rho5p* as a positive regulator of the fMAPK pathway.

Discussion

Signaling pathways can regulate the activity of transcription factors that control the expression of many genes that collectively generate cellular responses. To have a full understanding of the cellular responses a pathway generates, one must characterize the functions of individual targets of the signaling pathway. Here, we characterized targets of the fMAPK pathway in *S. cerevisiae*. This led to the discovery that, even though the fMAPK pathway overwhelmingly regulates filamentous growth positively, the pathway can also negatively regulate or modulate filamentous growth under some conditions. This also led to the discovery of new positive roles for the pathway in controlling cell adhesion and the cell cycle (Figure 8). In addition, by trying to identify how the target *RGD2* regulates invasive growth, we uncovered that *RHO5* positively regulates the fMAPK pathway (Figure 8).

A major role of the fMAPK pathway is to positively regulate invasive growth (Roberts and Fink 1994; Cook *et al.* 1997; Roberts *et al.* 2000; Cullen and Sprague 2012). Here, we show that the fMAPK pathway also negatively regulates invasive growth. This occurred under certain conditions by

1587
1588
1589
1590
1591
1592
1593
1594
1595
1596
1597
1598
1599
1600
1601
1602
1603
1604
1605
1606
1607
1608
1609
1610
1611
1612
1613
1614
1615
1616
1617
1618
1619
1620
1621
1622
1623
1624
1625
1626
1627
1628
1629
1630
1631
1632
1633
1634
1635
1636
1637
1638
1639
1640
1641
1642

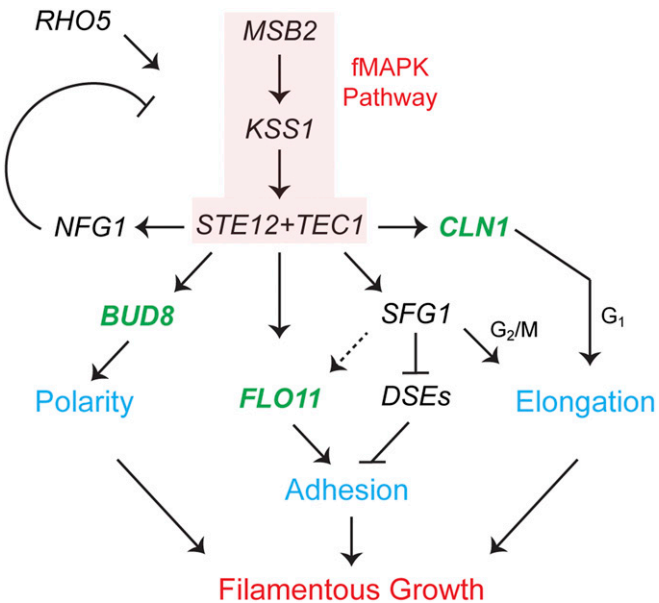


Figure 8 Model of how newly identified targets of the fMAPK pathway impact cell adhesion and cell elongation during filamentous growth. *Nfg1p* negatively regulates the fMAPK pathway. Other targets also negatively regulate filamentous growth (not shown). The fMAPK pathway induces cell adhesion by regulating *Flo11* expression, in part through *Sfg1p*, and by preventing cell separation through *Sfg1p*-dependent repression of *DSEs* and *SCW11*. The fMAPK pathway induces cell elongation by regulating the G_1 -specific cyclin *CLN1* and *SFG1*, which promotes extension of G_2/M . *Rho5p* regulates the fMAPK pathway. Pathway components are highlighted in red (*MSB2*, *KSS1*, *STE12*, *TEC1*).

regulating the expression of *NFG1*, *RGD2*, *RPI1*, and *TIP1*. Moreover, the fMAPK pathway induces the expression of these negative regulators to modulate the formation of invasive aggregates. This adds four new proteins to the large group of proteins that negatively regulate filamentous growth, including *Sfl1p* (Fujita *et al.* 1989; Robertson and Fink 1998; Song and Carlson 1998; Pan and Heitman 2002), *Nrg1p* (Park *et al.* 1999; Zhou and Winston 2001; Kuchin *et al.* 2002), *Sok2p* (Ward *et al.* 1995; Pan and Heitman 2000, 2002), and *Dig1p* (Cook *et al.* 1996; Tedford *et al.* 1997; Bardwell *et al.* 1998b; Olson *et al.* 2000). *Rgd2p*, *Rpi1p*, and *Tip1p* are conserved in several yeast species, including pathogens, and might have similar functions in these species. *Nfg1p*, however, only has homology within *Saccharomyces* yeast. Perhaps *Nfg1p* aids in a specific aspect of *Saccharomyces* ecology not found in other fungi.

Because the fMAPK pathway is involved in both the negative and positive regulation of filamentous growth, it implies the importance of fine tuning in the regulation of this response. Modulation ensures cells do not “overdo” filamentous growth, which, in some environments, could have negative impacts. For example, when *Dig1p* is overexpressed, it gives cells a growth advantage in liquid cultures, but reduces growth on semisolid surface (Tan *et al.* 2013). Furthermore,

a *dig1Δ* mutant has decreased biofilm/mat expansion (Karunanithi *et al.* 2012), which could make it more difficult to scavenge nutrients. Finally, elevated levels of *Flo11p*, although beneficial for invasive growth, dampens biofilm/mat expansion (Karunanithi *et al.* 2010).

Nfg1p has been an established, highly induced target of the fMAPK pathway with a function that has remained elusive for some time [*YLR042c*, (Caro *et al.* 1997; Hamada *et al.* 1999; Madhani *et al.* 1999; Roberts *et al.* 2000; Giaever *et al.* 2002; Hohmann 2002; García *et al.* 2004; Kim and Levin 2010; Parachin *et al.* 2010; Adhikari and Cullen 2014; Chow *et al.* 2019b)]. Here, we show *Nfg1p* regulates invasive growth by dampening the activity of the fMAPK pathway (Figure 8). This fits a common theme among some pathway targets that are induced to dampen pathway activity, resulting in negative feedback (Borneman *et al.* 2006). *Rgd2p*, *Rpi1p*, and *Tip1p* act at least somewhat separately from *Nfg1p* and each other to modulate invasive growth. *Rgd2p*, *Rpi1p*, and *Tip1p* may dampen other pathways that regulate filamentous growth (Gimeno *et al.* 1992; Lorenz and Heitman 1998; Carlson 1999; Pan and Heitman 1999; Cullen and Sprague 2000, 2012; Crespo *et al.* 2002; Lamb and Mitchell 2003) because intensive cross regulation between pathways occurs in a complex regulatory network (Bharucha *et al.* 2008; Chavel *et al.* 2010; et al. 2014; Chow *et al.* 2019b). As currently appreciated, it is not clear how signal amplification is curbed in the network. Here, we provide a possible explanation for this, by pathways making products that presumably dampen the activity of other pathways from the signaling network. For example, the fMAPK pathway may target *RPI1* because it dampens the Ras/cyclic AMP pathway (Kim and Powers 1991; Sobering *et al.* 2002), which also regulates filamentous growth (Mosch *et al.* 1996; Pan and Heitman 1999; Rupp *et al.* 1999; Cullen and Sprague 2012).

We also show that the transcriptional repressor *SFG1* is a target of the fMAPK pathway. *Sfg1p* regulates an entire filamentation program—it prevents cell separation by repressing genes encoding daughter-cell-wall degrading enzymes, it triggers cell cycle delay resulting in an elongated cell morphology, and it induces *Flo11* expression (Figure 8). *Sfg1p* also regulates cell adhesion separate from *Flo11p*. Thus, the regulation of *SFG1* expression by the fMAPK pathway identifies a new mechanism by which the fMAPK pathway regulates cell adhesion. *Sfg1p* and *Flo11p* do not always contribute equally to cell-adhesion responses, and cell-adhesion regulation by both proteins was affected by the environment. *Flo11p* regulated cell adhesion more intensely on semisolid than in liquid media, and both *Sfg1p* and *Flo11p* regulated invasive growth differently depending on the carbon source present. These new conditional mechanisms indicate that cell adhesion regulation is more complex than currently appreciated and suggests that, in yeast, there is an ‘adhesion code’. For example, we show here that the adhesion code is dependent on the regulation of adhesion molecules, cell-wall-degrading enzymes, and transcription factors, which are controlled differentially depending on

- the environment. Given the large number of adhesion molecules in *C. albicans* and other species (Tronchin *et al.* 1991; Brandhorst *et al.* 1999; Sheppard *et al.* 2004; Dranginis *et al.* 2007; Linder and Gustafsson 2008; Younes *et al.* 2011; de Groot *et al.* 2013; Lipke 2018; Takahashi-Nakaguchi *et al.* 2018), it is likely that the adhesion code in other species is similarly (or more) complex.
- Sfg1p* also regulated cell elongation, and based on previous work has been shown to induce a delay in G₂/M (White *et al.* 2009). Overall, it appears the fMAPK pathway integrates separate regulatory modes of filamentous growth into one response: (1) regulating cell adhesion by repressing the expression of genes that encode proteins involved in cell separation and inducing the expression of *FLO11* and (2) regulating the cell cycle at G₁ through *CLN1* and G₂ through *SFG1* to promote cell elongation (Figure 8). Having multiple mechanisms to regulate the same response increases the fine tuning capabilities of the pathway, making slight adjustments for different environments possible. *Sfg1p* is conserved across some species of yeast, including pathogens like *C. glabrata*, and could represent an important regulator of filamentous growth that leads to nuanced responses in other species.
- In conclusion, by characterizing transcriptional targets of the fMAPK pathway, we have identified novel roles for the pathway in regulating invasive growth, cell adhesion, and the cell cycle. Some of these mechanisms may be conserved in pathogenic yeasts and could assist in understanding fungal infections. Here, we focused on highly induced targets of the fMAPK pathway; however, there are many other target genes that are induced at lower levels that could impact phenotype. Moreover, there are also many targets whose expression is repressed that may tell us phenotypic information about the fMAPK pathway if explored. Overall, these findings suggest characterizing the genetic targets of other signaling pathways could lead to important advances in understanding signal transduction regulation.
- ## Acknowledgments
- Thanks to Kathryn Vandermeulen, Alexander Bowitch, and past and current laboratory members. The work was supported by a grant from the National Institutes of Health (NIH) (GM098629). The authors have no competing interests in the study.
- Author contributions: M.D.V. designed experiments, generated data, and wrote the paper; P.J.C. designed experiments, wrote the paper, and obtained funding.
- ## Literature Cited
- Adhikari, H., and P. J. Cullen, 2014 Metabolic respiration induces AMPK- and Ire1p-dependent activation of the p38-Type HOG MAPK pathway. *PLoS Genet.* 10: e1004734. <https://doi.org/10.1371/journal.pgen.1004734>
- Ahn, S. H., A. Acurio, and S. J. Kron, 1999 Regulation of G2/M progression by the STE mitogen-activated protein kinase pathway in budding yeast filamentous growth. *Mol. Biol. Cell* 10: 3301–3316. <https://doi.org/10.1091/mbc.10.10.3301>
- Annan, R. B., C. Wu, D. D. Waller, M. Whiteway, and D. Y. Thomas, 2008 Rho5p is involved in mediating the osmotic stress response in *Saccharomyces cerevisiae*, and its activity is regulated via Msi1p and Npr1p by phosphorylation and ubiquitination. *Eukaryot. Cell* 7: 1441–1449. <https://doi.org/10.1128/EC.00120-08>
- Aramayo, R., Y. Peleg, R. Addison, and R. Metzenberg, 1996 Asm1+, a *Neurospora crassa* gene related to transcriptional regulators of fungal development. *Genetics* 144: 991–1003.
- Azeredo, J., N. F. Azevedo, R. Briandet, N. Cerca, T. Coenye *et al.*, 2017 Critical review on biofilm methods. *Crit. Rev. Microbiol.* 43: 313–351. <https://doi.org/10.1080/1040841X.2016.1208146>
- Baladrón, V., S. Ufano, E. Duenas, A. B. Martin-Cuadrado, F. del Rey *et al.*, 2002 Eng1p, an endo-1,3-beta-glucanase localized at the daughter side of the septum, is involved in cell separation in *Saccharomyces cerevisiae*. *Eukaryot. Cell* 1: 774–786. <https://doi.org/10.1128/EC.15.774-786.2002>
- Bardwell, L., J. G. Cook, D. Voora, D. M. Baggott, A. R. Martinez *et al.*, 1998a Repression of yeast Ste12 transcription factor by direct binding of unphosphorylated Kss1 MAPK and its regulation by the Ste7 MEK. *Genes Dev.* 12: 2887–2898. <https://doi.org/10.1101/gad.12.18.2887>
- Bardwell, L., J. G. Cook, J. X. Zhu-Shimoni, D. Voora, and J. Thorner, 1998b Differential regulation of transcription: repression by unactivated mitogen-activated protein kinase Kss1 requires the Dig1 and Dig2 proteins. *Proc. Natl. Acad. Sci. USA* 95: 15400–15405. <https://doi.org/10.1073/pnas.95.26.15400>
- Barua, S., L. Li, P. N. Lipke, and A. M. Dranginis, 2016 Molecular basis for strain variation in the *Saccharomyces cerevisiae* adhesin Flo11p. *MSphere* 1: e00129–16. <https://doi.org/10.1128/mSphere.00129-16>
- Basu, S., N. Vadaie, A. Prabhakar, B. Li, H. Adhikari *et al.*, 2016 Spatial landmarks regulate a Cdc42-dependent MAPK pathway to control differentiation and the response to positional compromise. *Proc. Natl. Acad. Sci. USA* 113: E2019–E2028. <https://doi.org/10.1073/pnas.1522679113>
- Basu, S., B. Gonzalez, B. Li, G. Kimble, K. G. Kozminski *et al.*, 2020 Functions for Cdc42p BEM adaptors in regulating a differentiation-type MAP kinase pathway. *Mol. Biol. Cell* 31: 491–510. <https://doi.org/10.1091/mbc.E19-08-0441>
- Bharucha, N., J. Ma, C. J. Dobry, S. K. Lawson, Z. Yang *et al.*, 2008 Analysis of the yeast genome reveals a network of regulated protein localization during filamentous growth. *Mol. Biol. Cell* 19: 2708–2717. <https://doi.org/10.1091/mbc.e07-11-1199>
- Birkaya, B., A. Maddi, J. Joshi, S. J. Free, and P. J. Cullen, 2009 Role of the cell wall integrity and filamentous growth mitogen-activated protein kinase pathways in cell wall remodeling during filamentous growth. *Eukaryot. Cell* 8: 1118–1133. <https://doi.org/10.1128/EC.00006-09>
- Borneman, A. R., J. A. Leigh-Bell, H. Yu, P. Bertone, M. Gerstein *et al.*, 2006 Target hub proteins serve as master regulators of development in yeast. *Genes Dev.* 20: 435–448. <https://doi.org/10.1101/gad.1389306>
- Borneman, A. R., Z. D. Zhang, J. Rozowsky, M. R. Seringhaus, M. Gerstein *et al.*, 2007 Transcription factor binding site identification in yeast: a comparison of high-density oligonucleotide and PCR-based microarray platforms. *Funct. Integr. Genomics* 7: 335–345. <https://doi.org/10.1007/s10142-007-0054-7>
- Brandhorst, T. T., M. Wuthrich, T. Warner, and B. Klein, 1999 Targeted gene disruption reveals an adhesin indispensable for pathogenicity of *Blastomyces dermatitidis*. *J. Exp. Med.* 189: 1207–1216. <https://doi.org/10.1084/jem.189.8.1207>

- 1867 Brito, A. S., B. Neuhauser, R. Wintjens, A. M. Marini, and M. Boeck-
1868 staens, 2020 Yeast filamentation signaling is connected to a
1869 specific substrate translocation mechanism of the Mep2 trans-
1870 ceptor. *PLoS Genet.* 16: e1008634. <https://doi.org/10.1371/journal.pgen.1008634> 1923
1871 Brückner, S., R. Schubert, T. Kraushaar, R. Hartmann, D. Hoffmann
1872 et al., 2020 Kin discrimination in social yeast is mediated by
1873 cell surface receptors of the Flo11 adhesin family. *eLife* 9:
1874 e55587. <https://doi.org/10.7554/eLife.55587> 1924
1875 Byrne, K. P., and K. H. Wolfe, 2005 The Yeast Gene Order
1876 Browser: combining curated homology and synteny context re-
1877 veals gene fate in polyploid species. *Genome Res.* 15: 1456–
1878 1461. <https://doi.org/10.1101/gr.367230> 1925
1879 Byrne, K. P., and K. H. Wolfe, 2006 Visualizing synteny rela-
1880 tionships among the hemiascomycetes with the yeast gene order
1881 browser. *Nucleic Acids Res.* 34: D452–D455. <https://doi.org/10.1093/nar/gkj041> 1926
1882 Carlson, M., 1999 Glucose repression in yeast. *Curr. Opin. Micro-
1883 biol.* 2: 202–207. [https://doi.org/10.1016/S1369-5274\(99\)80035-6](https://doi.org/10.1016/S1369-5274(99)80035-6) 1927
1884 Carlson, M., B. C. Osmond, and D. Botstein, 1981 Mutants of
1885 yeast defective in sucrose utilization. *Genetics* 98: 25–40. 1928
1886 Caro, L. H., H. Tettelin, J. H. Vossen, A. F. Ram, H. van den Ende
1887 et al., 1997 In silicio identification of glycosyl-phosphatidyl-
1888 inositol-anchored plasma-membrane and cell wall proteins of
1889 *Saccharomyces cerevisiae*. *Yeast* 13: 1477–1489. [https://doi.org/10.1002/\(SICI\)1097-0061\(199712\)13:15<1477::AID-YEA184>3.0.CO;2-L](https://doi.org/10.1002/(SICI)1097-0061(199712)13:15<1477::AID-YEA184>3.0.CO;2-L) 1929
1890 Chang, L., and M. Karin, 2001 Mammalian MAP kinase signalling
1891 cascades. *Nature* 410: 37–40. <https://doi.org/10.1038/35065000> 1930
1892 Chavel, C. A., H. M. Dionne, B. Birkaya, J. Joshi, and P. J. Cullen,
1893 2010 Multiple signals converge on a differentiation MAPK
1894 pathway. *PLoS Genet.* 6: e1000883. <https://doi.org/10.1371/journal.pgen.1000883> 1931
1895 Chavel, C. A., L. M. Caccamise, B. Li, and P. J. Cullen, 2014 Global
1896 regulation of a differentiation MAPK pathway in yeast. *Genetics*
1897 198: 1309–1328. <https://doi.org/10.1534/genetics.114.168252> 1932
1898 Chen, H., and G. R. Fink, 2006 Feedback control of morphogen-
1899 esis in fungi by aromatic alcohols. *Genes Dev.* 20: 1150–1161.
1900 <https://doi.org/10.1101/gad.1411806> 1933
1901 Chin, B. L., O. Ryan, F. Lewitter, C. Boone, and G. R. Fink,
1902 2012 Genetic variation in *Saccharomyces cerevisiae*: circuit
1903 diversification in a signal transduction network. *Genetics* 192:
1904 1523–1532. <https://doi.org/10.1534/genetics.112.145573> 1934
1905 Chou, S., S. Lane, and H. Liu, 2006 Regulation of mating and
1906 filamentation genes by two distinct Ste12 complexes in *Saccha-*
1907 *romyces cerevisiae*. *Mol. Cell. Biol.* 26: 4794–4805. <https://doi.org/10.1128/MCB.02053-05> 1935
1908 Chow, J., M. Notaro, A. Prabhakar, S. J. Free, and P. J. Cullen,
1909 2018 Impact of fungal MAPK pathway targets on the cell wall.
1910 *J. Fungi (Basel)* 4: 93. <https://doi.org/10.3390/jof4030093> 1936
1911 Chow, J., H. M. Dionne, A. Prabhakar, A. Mehrotra, J. Somboon-
1912 thum et al., 2019a Aggregate filamentous growth responses in
1913 yeast. *MSphere* 4: e00702–18. <https://doi.org/10.1128/mSphere.00702-18> 1937
1914 Chow, J., I. Starr, S. Jamalzadeh, O. Muniz, A. Kumar et al.,
1915 2019b Filamentation regulatory pathways control adhesion-
1916 dependent surface responses in yeast. *Genetics* 212: 667–690.
1917 <https://doi.org/10.1534/genetics.119.302004> 1938
1918 Cook, J. G., L. Bardwell, S. J. Kron, and J. Thorner, 1996 Two
1919 novel targets of the MAP kinase Kss1 are negative regulators of
1920 invasive growth in the yeast *Saccharomyces cerevisiae*. *Genes*
1921 *Dev.* 10: 2831–2848. <https://doi.org/10.1101/gad.10.22.2831> 1939
1922 Cook, J. G., L. Bardwell, and J. Thorner, 1997 Inhibitory and
activating functions for MAPK Kss1 in the *S. cerevisiae* filamen-
tous-growth signalling pathway. *Nature* 390: 85–88. <https://doi.org/10.1038/36355> 1940
Costanzo, M., A. Baryshnikova, J. Bellay, Y. Kim, E. D. Spear et al.,
2010 The genetic landscape of a cell. *Science* 327: 425–431.
<https://doi.org/10.1126/science.1180823> 1941
Costerton, J. W., P. S. Stewart, and E. P. Greenberg, 1999 Bacterial biofilms: a common cause of persistent infections. *Science* 284: 1318–1322. <https://doi.org/10.1126/science.284.5418.1318> 1942
Courchesne, W. E., R. Kunisawa, and J. Thorner, 1989 A putative
protein kinase overcomes pheromone-induced arrest of cell cycl-
ing in *S. cerevisiae*. *Cell* 58: 1107–1119. [https://doi.org/10.1016/0092-8674\(89\)90509-6](https://doi.org/10.1016/0092-8674(89)90509-6) 1943
Craig Maclean, R., and C. Brandon, 2008 Stable public goods co-
operation and dynamic social interactions in yeast. *J. Evol. Biol.*
21: 1836–1843. <https://doi.org/10.1111/j.1420-9101.2008.01579.x> 1944
Crespo, J. L., T. Powers, B. Fowler, and M. N. Hall, 2002 The
TOR-controlled transcription activators GLN3, RTG1, and
RTG3 are regulated in response to intracellular levels of glutama-
tine. *Proc. Natl. Acad. Sci. USA* 99: 6784–6789. <https://doi.org/10.1073/pnas.102687599> 1945
Csank, C., and K. Haynes, 2000 *Candida glabrata* displays pseu-
dohyphal growth. *FEMS Microbiol. Lett.* 189: 115–120. <https://doi.org/10.1111/j.1574-6968.2000.tb09216.x> 1946
Cullen, P. J., 2015 The plate-washing assay: a simple test for
filamentous growth in budding yeast. *Cold Spring Harb. Protoc.*
2015: 168–171. <https://doi.org/10.1101/pdb.prot085068> 1947
Cullen, P. J., and G. F. Sprague, Jr., 2000 Glucose depletion
causes haploid invasive growth in yeast. *Proc. Natl. Acad. Sci.*
USA 97: 13619–13624. <https://doi.org/10.1073/pnas.240345197> 1948
Cullen, P. J., and G. F. Sprague, Jr., 2002 The roles of bud-site-
selection proteins during haploid invasive growth in yeast. *Mol.*
Biol. Cell 13: 2990–3004. <https://doi.org/10.1091/mbc.e02-03-0151> 1949
Cullen, P. J., and G. F. Sprague, Jr., 2012 The regulation of fila-
mentous growth in yeast. *Genetics* 190: 23–49. <https://doi.org/10.1534/genetics.111.127456> 1950
Cullen, P. J., J. Schultz, J. Horecka, B. J. Stevenson, Y. Jigami et al.,
2000 Defects in protein glycosylation cause SHO1-dependent
activation of a STE12 signaling pathway in yeast. *Genetics* 155:
1005–1018. 1951
Cullen, P. J., W. Sabbagh, Jr., E. Graham, M. M. Irick, E. K. van
Olden et al., 2004 A signaling mucin at the head of the Cdc42-
and MAPK-dependent filamentous growth pathway in yeast.
Genes Dev. 18: 1695–1708. <https://doi.org/10.1101/gad.1178604> 1952
de Groot, P. W., O. Bader, A. D. de Boer, M. Weig, and N. Chauhan,
2013 Adhesins in human fungal pathogens: glue with plenty
of stick. *Eukaryot. Cell* 12: 470–481. <https://doi.org/10.1128/EC.00364-12> 1953
Doolin, M. T., A. L. Johnson, L. H. Johnston, and G. Butler,
2001 Overlapping and distinct roles of the duplicated yeast
transcription factors Ace2p and Swi5p. *Mol. Microbiol.* 40:
422–432. <https://doi.org/10.1046/j.1365-2958.2001.02388.x> 1954
Dranginis, A. M., J. M. Rauseo, J. E. Coronado, and P. N. Lipke,
2007 A biochemical guide to yeast adhesins: glycoproteins for
social and antisocial occasions. *Microbiol. Mol. Biol. Rev.* 71:
282–294. <https://doi.org/10.1128/MMBR.00037-06> 1955
Draper, E., O. Dubrovsky, E. E. Bar, and D. E. Stone, 2009 Dse1
may control cross talk between the pheromone and filamentation
pathways in yeast. *Curr. Genet.* 55: 611–621. <https://doi.org/10.1007/s00294-009-0274-6> 1956
Edgington, N. P., M. J. Blacketer, T. A. Bierwagen, and A. M. Myers,
1999 Control of *Saccharomyces cerevisiae* filamentous growth 1957
1958

- 1979 by cyclin-dependent kinase Cdc28. *Mol. Cell. Biol.* 19: 1369–1380. <https://doi.org/10.1128/MCB.19.2.1369>
- 1980 Fidalgo, M., R. R. Barrales, J. I. Ibeas, and J. Jimenez, 2006 Adaptive evolution by mutations in the FLO11 gene. *Proc. Natl. Acad. Sci. USA* 103: 11228–11233. <https://doi.org/10.1073/pnas.0601713103>
- 1981 Fidel, Jr., P. L., J. A. Vazquez, and J. D. Sobel, 1999 *Candida glabrata*: review of epidemiology, pathogenesis, and clinical disease with comparison to *C. albicans*. *Clin. Microbiol. Rev.* 12: 80–96. <https://doi.org/10.1128/CMR.12.1.80>
- 1982 Flatauer, L. J., S. F. Zadeh, and L. Bardwell, 2005 Mitogen-activated protein kinases with distinct requirements for Ste5 scaffolding influence signaling specificity in *Saccharomyces cerevisiae*. *Mol. Cell. Biol.* 25: 1793–1803. <https://doi.org/10.1128/MCB.25.5.1793-1803.2005>
- 1983 Flemming, H. C., and J. Wingender, 2010 The biofilm matrix. *Nat. Rev. Microbiol.* 8: 623–633. <https://doi.org/10.1038/nrmicro2415>
- 1984 Foster, H. A., M. Cui, A. Naveenathayalan, H. Unden, R. Schwanbeck *et al.*, 2013 The zinc cluster protein Sut1 contributes to filamentation in *Saccharomyces cerevisiae*. *Eukaryot. Cell* 12: 244–253. <https://doi.org/10.1128/EC.00214-12>
- 1985 Fujii, T., H. Shimoji, and Y. Iimura, 1999 Structure of the glucan-binding sugar chain of Tip1p, a cell wall protein of *Saccharomyces cerevisiae*. *Biochim. Biophys. Acta* 1427: 133–144. [https://doi.org/10.1016/S0304-4165\(99\)00012-4](https://doi.org/10.1016/S0304-4165(99)00012-4)
- 1986 Fujita, A., Y. Kikuchi, S. Kuhara, Y. Misumi, S. Matsumoto *et al.*, 1989 Domains of the SFL1 protein of yeasts are homologous to Myc oncoproteins or yeast heat-shock transcription factor. *Gene* 85: 321–328. [https://doi.org/10.1016/0378-1119\(89\)90424-1](https://doi.org/10.1016/0378-1119(89)90424-1)
- 1987 Fujita, A., T. Hiroko, F. Hiroko, and C. Oka, 2005 Enhancement of superficial pseudohyphal growth by overexpression of the SFG1 gene in yeast *Saccharomyces cerevisiae*. *Gene* 363: 97–104. <https://doi.org/10.1016/j.gene.2005.06.036>
- 1988 García, R., C. Bermejo, C. Grau, R. Perez, J. M. Rodriguez-Pena *et al.*, 2004 The global transcriptional response to transient cell wall damage in *Saccharomyces cerevisiae* and its regulation by the cell integrity signaling pathway. *J. Biol. Chem.* 279: 15183–15195. <https://doi.org/10.1074/jbc.M312954200>
- 1989 Garcia-Ranea, J. A., and A. Valencia, 1998 Distribution and functional diversification of the ras superfamily in *Saccharomyces cerevisiae*. *FEBS Lett.* 434: 219–225. [https://doi.org/10.1016/S0014-5793\(98\)00967-3](https://doi.org/10.1016/S0014-5793(98)00967-3)
- 1990 Gelperin, D. M., M. A. White, M. L. Wilkinson, Y. Kon, L. A. Kung *et al.*, 2005 Biochemical and genetic analysis of the yeast proteome with a movable ORF collection. *Genes Dev.* 19: 2816–2826. <https://doi.org/10.1101/gad.1362105>
- 1991 Giaever, G., A. M. Chu, L. Ni, C. Connelly, L. Riles *et al.*, 2002 Functional profiling of the *Saccharomyces cerevisiae* genome. *Nature* 418: 387–391. <https://doi.org/10.1038/nature00935>
- 1992 Gietz, R. D., 2014 Yeast transformation by the LiAc/SS carrier DNA/PEG method. *Methods Mol. Biol.* 1205: 1–12. https://doi.org/10.1007/978-1-4939-1363-3_1
- 1993 Gimeno, C. J., and G. R. Fink, 1994 Induction of pseudohyphal growth by overexpression of PHD1, a *Saccharomyces cerevisiae* gene related to transcriptional regulators of fungal development. *Mol. Cell. Biol.* 14: 2100–2112. <https://doi.org/10.1128/MCB.14.3.2100>
- 1994 Gimeno, C. J., P. O. Ljungdahl, C. A. Styles, and G. R. Fink, 1992 Unipolar cell divisions in the yeast *S. cerevisiae* lead to filamentous growth: regulation by starvation and RAS. *Cell* 68: 1077–1090. [https://doi.org/10.1016/0092-8674\(92\)90079-R](https://doi.org/10.1016/0092-8674(92)90079-R)
- 1995 González, B., A. Mas, G. Beltran, P. J. Cullen, and M. J. Torija, 2017 Role of mitochondrial retrograde pathway in regulating ethanol-inducible filamentous growth in yeast. *Front. Physiol.* 8: 148. <https://doi.org/10.3389/fphys.2017.00148>
- 1996 Granek, J. A., and P. M. Magwene, 2010 Environmental and genetic determinants of colony morphology in yeast. *PLoS Genet.* 6: e1000823. <https://doi.org/10.1371/journal.pgen.1000823>
- 1997 Greig, D., and M. Travisano, 2004 The Prisoner's Dilemma and polymorphism in yeast SUC genes. *Proc. Biol. Sci.* 271: S25–S26. <https://doi.org/10.1098/rsbl.2003.0083>
- 1998 Guo, B., C. A. Styles, Q. Feng, and G. R. Fink, 2000 A *Saccharomyces* gene family involved in invasive growth, cell-cell adhesion, and mating. *Proc. Natl. Acad. Sci. USA* 97: 12158–12163. <https://doi.org/10.1073/pnas.220420397>
- 1999 Hadwiger, J. A., C. Wittenberg, H. E. Richardson, M. de Barros Lopes, and S. I. Reed, 1989 A family of cyclin homologs that control the G1 phase in yeast. *Proc. Natl. Acad. Sci. USA* 86: 6255–6259. <https://doi.org/10.1073/pnas.86.16.6255>
- 2000 Halme, A., S. Bumgarner, C. Styles, and G. R. Fink, 2004 Genetic and epigenetic regulation of the FLO gene family generates cell-surface variation in yeast. *Cell* 116: 405–415. [https://doi.org/10.1016/S0092-8674\(04\)00118-7](https://doi.org/10.1016/S0092-8674(04)00118-7)
- 2001 Hamada, K., H. Terashima, M. Arisawa, N. Yabuki, and K. Kitada, 1999 Amino acid residues in the omega-minus region participate in cellular localization of yeast glycosylphosphatidylinositol-attached proteins. *J. Bacteriol.* 181: 3886–3889. <https://doi.org/10.1128/JB.181.13.3886-3889.1999>
- 2002 Harbison, C. T., D. B. Gordon, T. I. Lee, N. J. Rinaldi, K. D. Macisaac *et al.*, 2004 Transcriptional regulatory code of a eukaryotic genome. *Nature* 431: 99–104. <https://doi.org/10.1038/nature02800>
- 2003 Heise, B., J. van der Felden, S. Kern, M. Malcher, S. Bruckner *et al.*, 2010 The TEA transcription factor Tec1 confers promoter-specific gene regulation by Ste12-dependent and -independent mechanisms. *Eukaryot. Cell* 9: 514–531. <https://doi.org/10.1128/EC.00251-09>
- 2004 Hohmann, S., 2002 Osmotic stress signaling and osmoadaptation in yeasts. *Microbiol. Mol. Biol. Rev.* 66: 300–372. <https://doi.org/10.1128/MMBR.66.2.300-372.2002>
- 2005 Jarvis, E. E., D. C. Hagen, and G. F. Sprague, Jr., 1988 Identification of a DNA segment that is necessary and sufficient for alpha-specific gene control in *Saccharomyces cerevisiae*: implications for regulation of alpha-specific and a-specific genes. *Mol. Cell. Biol.* 8: 309–320. <https://doi.org/10.1128/MCB.8.1.309>
- 2006 Kabir, M. A., M. A. Hussain, and Z. Ahmad, 2012 *Candida albicans*: a model organism for studying fungal pathogens. *ISRN Microbiol.* 2012: 538694. <https://doi.org/10.5402/2012/538694>
- 2007 Karunanthithi, S., and P. J. Cullen, 2012 The filamentous growth MAPK pathway responds to glucose starvation through the mig1/2 transcriptional repressors in *Saccharomyces cerevisiae*. *Genetics* 192: 869–887. <https://doi.org/10.1534/genetics.112.142661>
- 2008 Karunanthithi, S., N. Vadaie, C. A. Chavel, B. Birkaya, J. Joshi *et al.*, 2010 Shedding of the mucin-like flocculin Flo11p reveals a new aspect of fungal adhesion regulation. *Curr. Biol.* 20: 1389–1395. <https://doi.org/10.1016/j.cub.2010.06.033>
- 2009 Karunanthithi, S., J. Joshi, C. Chavel, B. Birkaya, L. Grell *et al.*, 2012 Regulation of mat responses by a differentiation MAPK pathway in *Saccharomyces cerevisiae*. *PLoS One* 7: e32294. <https://doi.org/10.1371/journal.pone.0032294>
- 2010 Kennedy, M. J., A. L. Rogers, and R. J. Yancey, Jr., 1989 Environmental alteration and phenotypic regulation of *Candida albicans* adhesion to plastic. *Infect. Immun.* 57: 3876–3881. <https://doi.org/10.1128/IAI.57.12.3876-3881.1989>
- 2011 Kim, J. H., and S. Powers, 1991 Overexpression of RPI1, a novel inhibitor of the yeast Ras-cyclic AMP pathway, down-regulates normal but not mutationally activated ras function. *Mol. Cell. Biol.* 11: 3894–3904. <https://doi.org/10.1128/MCB.11.8.3894>

- 2091 Kim, K. Y., and D. E. Levin, 2010 Transcriptional reporters for
2092 genes activated by cell wall stress through a non-catalytic mech-
2093 anism involving Mpk1 and SBF. *Yeast* 27: 541–548. <https://doi.org/10.1002/yea.1782> 2147
2094 King, L., and G. Butler, 1998 Ace2p, a regulator of CTS1 (chiti-
2095 nase) expression, affects pseudohyphal production in *Saccharo-*
2096 *myes cerevisiae*. *Curr. Genet.* 34: 183–191. [https://doi.org/ 2148
2097 10.1007/s002940050384](https://doi.org/10.1007/s002940050384) 2149
2098 Kondo, K., and M. Inouye, 1991 TIP 1, a cold shock-inducible 2150
2099 gene of *Saccharomyces cerevisiae*. *J. Biol. Chem.* 266: 17537– 2151
17544. 2152
2100 Koschwanez, J. H., K. R. Foster, and A. W. Murray, 2011 Sucrose 2153
2101 utilization in budding yeast as a model for the origin of undif- 2154
2102 ferentiated multicellularity. *PLoS Biol.* 9: e1001122. [https://doi.org/ 2155
2103 10.1371/journal.pbio.1001122](https://doi.org/10.1371/journal.pbio.1001122) 2156
2104 Kraushaar, T., S. Bruckner, M. Veelders, D. Rhinow, F. Schreiner 2157
et al., 2015 Interactions by the fungal Flo11 adhesin depend 2158
on a fibronectin type III-like adhesin domain girdled by aromatic 2159
bands. *Structure* 23: 1005–1017. [https://doi.org/ 2160
2105 10.1016/j.str.2015.03.021](https://doi.org/10.1016/j.str.2015.03.021) 2161
2106 Kron, S. J., C. A. Styles, and G. R. Fink, 1994 Symmetric cell 2162
2107 division in pseudohyphae of the yeast *Saccharomyces cerevisiae*. 2163
Mol. Biol. Cell 5: 1003–1022. [https://doi.org/ 2164
2108 10.1091/mbc.5.9.1003](https://doi.org/10.1091/mbc.5.9.1003) 2165
2109 Kuchin, S., V. K. Vyas, and M. Carlson, 2002 Snf1 protein kinase 2166
2110 and the repressors Nrg1 and Nrg2 regulate FLO11, haploid invasive 2167
2111 growth, and diploid pseudohyphal differentiation. *Mol. Cell. Biol.* 22: 2168
3994–4000. [https://doi.org/ 2169
2112 10.1128/MCB.22.12.3994-4000.2002](https://doi.org/10.1128/MCB.22.12.3994-4000.2002) 2170
2113 Labbaoui, H., S. Bogliolo, V. Ghugtyal, N. V. Solis, S. G. Filler et al., 2171
2114 2017 Role of Arf GTPases in fungal morphogenesis and viru- 2172
2115 lence. *PLoS Pathog.* 13: e1006205. [https://doi.org/ 2173
2116 10.1371/journal.ppat.1006205](https://doi.org/10.1371/journal.ppat.1006205) 2174
2117 Laloux, I., E. Dubois, M. Dewerchin, and E. Jacobs, 1990 TEC1, a 2175
2118 gene involved in the activation of Ty1 and Ty1-mediated gene 2176
2119 expression in *Saccharomyces cerevisiae*: cloning and molecular 2177
2120 analysis. *Mol. Cell. Biol.* 10: 3541–3550. [https://doi.org/ 2178
2121 10.1128/MCB.10.7.3541](https://doi.org/10.1128/MCB.10.7.3541) 2179
2122 Lamb, T. M., and A. P. Mitchell, 2003 The transcription factor 2180
Rim101p governs ion tolerance and cell differentiation by direct 2181
2123 repression of the regulatory genes NRG1 and SMP1 in *Saccha-* 2182
2124 *romyes cerevisiae*. *Mol. Cell. Biol.* 23: 677–686. [https://doi.org/ 2183
2125 10.1128/MCB.23.2.677-686.2003](https://doi.org/10.1128/MCB.23.2.677-686.2003) 2184
2126 Lambrechts, M. G., F. F. Bauer, J. Marmur, and I. S. Pretorius, 2185
1996 Muc1, a mucin-like protein that is regulated by Mss10, 2186
2127 is critical for pseudohyphal differentiation in yeast. *Proc. Natl. 2187
Acad. Sci. USA* 93: 8419–8424. [https://doi.org/ 2188
2128 10.1073/pnas.93.16.8419](https://doi.org/10.1073/pnas.93.16.8419) 2189
2129 Lee, M. J., and H. G. Dohlman, 2008 Coactivation of G protein 2190
signaling by cell-surface receptors and an intracellular exchange 2191
factor. *Curr. Biol.* 18: 211–215. [https://doi.org/ 2192
2130 10.1016/j.cub.2008.01.007](https://doi.org/10.1016/j.cub.2008.01.007) 2193
2131 Lefrançois, P., G. M. Euskirchen, R. K. Auerbach, J. Rozowsky, T. 2194
Gibson et al., 2009 Efficient yeast ChIP-Seq using multiplex 2195
2132 short-read DNA sequencing. *BMC Genomics* 10: 37. [https://doi.org/ 2196
2133 10.1186/1471-2164-10-37](https://doi.org/10.1186/1471-2164-10-37) 2197
2134 Lenhart, B. A., B. Meeks, and H. A. Murphy, 2019 Variation in 2198
filamentous growth and response to quorum-sensing com- 2199
2135 pounds in environmental isolates of *Saccharomyces cerevisiae*. 2200
G3 (Bethesda) 9: 1533–1544. [https://doi.org/ 2201
2136 10.1534/g3.119.400080](https://doi.org/10.1534/g3.119.400080) 2202
2137 Linder, T., and C. M. Gustafsson, 2008 Molecular phylogenetics of
2138 ascomycotal adhesins—a novel family of putative cell-surface ad-
2139 hesive proteins in fission yeasts. *Fungal Genet. Biol.* 45: 485– 2140
497. [https://doi.org/ 2141
2142 10.1016/j.fgb.2007.08.002](https://doi.org/10.1016/j.fgb.2007.08.002)
- Lipke, P. N., 2018 What we do not know about fungal cell adhe-
2143 sion molecules. *J. Fungi (Basel)* 4: 59. [https://doi.org/ 2144
jof4020059](https://doi.org/10.3390/jof4020059) 2145
Liu, H., C. A. Styles, and G. R. Fink, 1993 Elements of the yeast 2146
pheromone response pathway required for filamentous growth 2147
of diploids. *Science* 262: 1741–1744. [https://doi.org/ 2148
10.1126/science.8259520](https://doi.org/10.1126/science.8259520) 2149
Lo, H. J., J. R. Kohler, B. DiDomenico, D. Loebenberg, A. Caccia- 2150
puoti et al., 1997 Nonfilamentous *C. albicans* mutants are avir- 2151
ulent. *Cell* 90: 939–949. [https://doi.org/ 2152
10.1016/S0092-8674\(00\)80358-X](https://doi.org/10.1016/S0092-8674(00)80358-X) 2153
Lo, W. S., and A. M. Dranginis, 1996 FLO11, a yeast gene related 2154
to the STA genes, encodes a novel cell surface flocculin. *J. Bacteriol.* 178: 7144–7151. [https://doi.org/ 2155
10.1128/JB.178.24.7144-7151.1996](https://doi.org/10.1128/JB.178.24.7144-7151.1996) 2156
Lo, W. S., and A. M. Dranginis, 1998 The cell surface flocculin 2157
Flo11 is required for pseudohyphae formation and invasion by 2158
Saccharomyces cerevisiae. *Mol. Biol. Cell* 9: 161–171. [https://doi.org/ 2159
10.1091/mbc.9.1.161](https://doi.org/10.1091/mbc.9.1.161) 2160
Loeb, J. D., T. A. Kerentseva, T. Pan, M. Sepulveda-Becerra, and H. 2161
Liu, 1999 *Saccharomyces cerevisiae* G1 cyclins are differen- 2162
tially involved in invasive and pseudohyphal growth indepen- 2163
dent of the filamentation mitogen-activated protein kinase 2164
pathway. *Genetics* 153: 1535–1546. 2165
Lorenz, M. C., and J. Heitman, 1998 The MEP2 ammonium per- 2166
mease regulates pseudohyphal differentiation in *Saccharomyces* 2167
cerevisiae. *EMBO J.* 17: 1236–1247. [https://doi.org/ 2168
10.1093/emboj/17.5.1236](https://doi.org/10.1093/emboj/17.5.1236) 2169
Madhani, H. D., T. Galitski, E. S. Lander, and G. R. Fink, 1999 2170
Effectors of a developmental mitogen-activated protein kinase 2171
cascade revealed by expression signatures of signaling 2172
mutants. *Proc. Natl. Acad. Sci. USA* 96: 12530–12535. 2173
<https://doi.org/10.1073/pnas.96.22.12530> 2174
Meem, M. H., and P. J. Cullen, 2012 The impact of protein gly- 2175
cosylation on Flo11-dependent adherence in *Saccharomyces* 2176
cerevisiae. *FEMS Yeast Res.* 12: 809–818. [https://doi.org/ 2177
10.1111/j.1567-1364.2012.00832.x](https://doi.org/10.1111/j.1567-1364.2012.00832.x) 2178
Miller, K. Y., J. Wu, and B. L. Miller, 1992 StuA is required for cell 2179
pattern formation in *Aspergillus*. *Genes Dev.* 6: 1770–1782. 2180
<https://doi.org/10.1101/gad.6.9.1770> 2181
Morrison, D. K., 2012 MAP kinase pathways. *Cold Spring Harb. 2182
Perspect. Biol.* 4: a011254. [https://doi.org/ 2183
10.1101/cshperspect.a011254](https://doi.org/10.1101/cshperspect.a011254) 2184
Mosch, H. U., R. L. Roberts, and G. R. Fink, 1996 Ras2 signals via 2185
the Cdc42/Ste20/mitogen-activated protein kinase module to 2186
induce filamentous growth in *Saccharomyces cerevisiae*. *Proc. Natl. 2187
Acad. Sci. USA* 93: 5352–5356. [https://doi.org/ 2188
10.1073/pnas.93.11.5352](https://doi.org/10.1073/pnas.93.11.5352) 2189
Mutlu, N., D. T. Sheidy, A. Hsu, H. S. Jeong, K. J. Wozniak et al., 2190
2019 A stress-responsive signaling network regulating pseudo- 2191
hyphal growth and ribonucleoprotein granule abundance in 2192
Saccharomyces cerevisiae. *Genetics* 213: 705–720. [https://doi.org/ 2193
10.1534/genetics.119.302538](https://doi.org/10.1534/genetics.119.302538) 2194
Ni, L., and M. Snyder, 2001 A genomic study of the bipolar bud 2195
site selection pattern in *Saccharomyces cerevisiae*. *Mol. Biol. Cell* 12: 2147–2170. [https://doi.org/ 2196
10.1091/mbc.12.7.2147](https://doi.org/10.1091/mbc.12.7.2147) 2197
Nobile, C. J., J. E. Nett, D. R. Andes, and A. P. Mitchell, 2006 2198
Function of *Candida albicans* adhesin Hwp1 in biofilm 2199
formation. *Eukaryot. Cell* 5: 1604–1610. [https://doi.org/ 2200
10.1128/EC.00194-06](https://doi.org/10.1128/EC.00194-06) 2201
Norman, K. L., C. A. Shively, A. J. De La Rocha, N. Mutlu, S. Basu 2202
et al., 2018 Inositol polyphosphates regulate and predict yeast 2203
pseudohyphal growth phenotypes. *PLoS Genet.* 14: e1007493. 2204
<https://doi.org/10.1371/journal.pgen.1007493> 2205
Olson, K. A., C. Nelson, G. Tai, W. Hung, C. Yong et al., 2000 Two 2206
regulators of Ste12p inhibit pheromone-responsive transcription 2207

- 2203 by separate mechanisms. *Mol. Cell. Biol.* 20: 4199–4209.
2204 <https://doi.org/10.1128/MCB.20.12.4199-4209.2000>
- 2205 Pan, X., and J. Heitman, 1999 Cyclic AMP-dependent protein ki-
2206 nase regulates pseudohyphal differentiation in *Saccharomyces*
2207 *cerevisiae*. *Mol. Cell. Biol.* 19: 4874–4887. <https://doi.org/10.1128/MCB.19.7.4874>
- 2208 Pan, X., and J. Heitman, 2000 Sok2 regulates yeast pseudohyphal
2209 differentiation via a transcription factor cascade that regulates
2210 cell-cell adhesion. *Mol. Cell. Biol.* 20: 8364–8372. <https://doi.org/10.1128/MCB.20.22.8364-8372.2000>
- 2211 Pan, X., and J. Heitman, 2002 Protein kinase A operates a molec-
2212 ular switch that governs yeast pseudohyphal differentiation.
2213 *Mol. Cell. Biol.* 22: 3981–3993. <https://doi.org/10.1128/MCB.22.12.3981-3993.2002>
- 2214 Parachin, N. S., O. Bengtsson, B. Hahn-Hagerdal, and M. F. Gorwa-
2215 Grauslund, 2010 The deletion of YLR042c improves ethanolic
2216 xylose fermentation by recombinant *Saccharomyces cerevisiae*.
2217 *Yeast* 27: 741–751. <https://doi.org/10.1002/yea.1777>
- 2218 Park, S. H., S. S. Koh, J. H. Chun, H. J. Hwang, and H. S. Kang,
2219 1999 Nrg1 is a transcriptional repressor for glucose repression
2220 of STA1 gene expression in *Saccharomyces cerevisiae*. *Mol. Cell.*
2221 *Biol.* 19: 2044–2050. <https://doi.org/10.1128/MCB.19.3.2044>
- 2222 Pitoniak, A., B. Birkaya, H. M. Dionne, N. Vadaie, and P. J. Cullen,
2223 2009 The signaling mucins Msb2 and Hkr1 differentially reg-
2224 ulate the filamentation mitogen-activated protein kinase path-
2225 way and contribute to a multimodal response. *Mol. Biol. Cell* 20:
2226 3101–3114. <https://doi.org/10.1091/mbc.e08-07-0760>
- 2227 Puria, R., M. A. Mannan, R. Chopra-Dewasthaly, and K. Ganesan,
2228 2009 Critical role of RPI1 in the stress tolerance of yeast dur-
2229 ing ethanolic fermentation. *FEMS Yeast Res.* 9: 1161–1171.
2230 <https://doi.org/10.1111/j.1567-1364.2009.00549.x>
- 2231 Reynolds, T. B., 2018 Going with the flo: the role of flo11-depen-
2232 dent and independent interactions in yeast Mat formation.
2233 *J. Fungi (Basel)* 4: 132. <https://doi.org/10.3390/jof4040132>
- 2234 Reynolds, T. B., and G. R. Fink, 2001 Bakers' yeast, a model for
2235 fungal biofilm formation. *Science* 291: 878–881. <https://doi.org/10.1126/science.291.5505.878>
- 2236 Roberts, C. J., B. Nelson, M. J. Marton, R. Stoughton, M. R. Meyer
2237 et al., 2000 Signaling and circuitry of multiple MAPK path-
2238 ways revealed by a matrix of global gene expression profiles.
2239 *Science* 287: 873–880. <https://doi.org/10.1126/science.287.5454.873>
- 2240 Roberts, R. L., and G. R. Fink, 1994 Elements of a single MAP
2241 kinase cascade in *Saccharomyces cerevisiae* mediate two devel-
2242 opmental programs in the same cell type: mating and invasive
2243 growth. *Genes Dev.* 8: 2974–2985. <https://doi.org/10.1101/gad.8.24.2974>
- 2244 Robertson, L. S., and G. R. Fink, 1998 The three yeast A kinases
2245 have specific signaling functions in pseudohyphal growth. *Proc.*
2246 *Natl. Acad. Sci. USA* 95: 13783–13787. <https://doi.org/10.1073/pnas.95.23.13783>
- 2247 Rodrigues, C. F., S. Silva, and M. Henriques, 2014 *Candida glab-*
2248 *rata*: a review of its features and resistance. *Eur. J. Clin. Micro-*
2249 *biol. Infect. Dis.* 33: 673–688. <https://doi.org/10.1007/s10096-013-2009-3>
- 2250 Roumanie, O., C. Weinachter, I. Larrieu, M. Crouzet, and F.
2251 Doignon, 2001 Functional characterization of the Bag7, Lrg1
2252 and Rggd2 RhoGAP proteins from *Saccharomyces cerevisiae*.
2253 *FEBS Lett.* 506: 149–156. [https://doi.org/10.1016/S0014-5793\(01\)02906-4](https://doi.org/10.1016/S0014-5793(01)02906-4)
- 2254 Rupp, S., E. Summers, H. J. Lo, H. Madhani, and G. Fink,
2255 1999 MAP kinase and cAMP filamentation signaling pathways
2256 converge on the unusually large promoter of the yeast FLO11
2257 gene. *EMBO J.* 18: 1257–1269. <https://doi.org/10.1093/emboj/18.5.1257>
- 2258 Ryan, O., R. S. Shapiro, C. F. Kurat, D. Mayhew, A. Baryshnikova
2259 et al., 2012 Global gene deletion analysis exploring yeast fila-
- 2260 mentous growth. *Science* 337: 1353–1356. <https://doi.org/10.1126/science.1224339>
- 2261 Sabbagh, Jr., W., L. J. Flatauer, A. J. Bardwell, and L. Bardwell,
2262 2001 Specificity of MAP kinase signaling in yeast differentia-
2263 tion involves transient vs. sustained MAPK activation. *Mol. Cell*
2264 8: 683–691. [https://doi.org/10.1016/S1097-2765\(01\)00322-7](https://doi.org/10.1016/S1097-2765(01)00322-7)
- 2265 Schmitz, H. P., A. Jendretzki, C. Sterk, and J. J. Heinisch,
2266 2018 The small yeast GTPase Rho5 and its dimeric GEF
2267 dck1/Lmo1 respond to glucose starvation. *Int. J. Mol. Sci.* 19:
2268 2186. <https://doi.org/10.3390/ijms19082186>
- 2269 Seger, R., 2010 *MAP Kinase Signaling Protocols*. Humana Press,
2270 New York. <https://doi.org/10.1007/978-1-60761-795-2>
- 2271 Seger, R., and E. G. Krebs, 1995 The MAPK signaling cascade.
2272 *FASEB J.* 9: 726–735. <https://doi.org/10.1096/fasebj.9.9.7601337>
- 2273 Sheppard, D. C., M. R. Yeaman, W. H. Welch, Q. T. Phan, Y. Fu
2274 et al., 2004 Functional and structural diversity in the Als pro-
2275 tein family of *Candida albicans*. *J. Biol. Chem.* 279: 30480–
2276 30489. <https://doi.org/10.1074/jbc.M401929200>
- 2277 Sikorski, R. S., and P. Hieter, 1989 A system of shuttle vectors and
2278 yeast host strains designed for efficient manipulation of DNA in
2279 *Saccharomyces cerevisiae*. *Genetics* 122: 19–27.
- 2280 Silva-Dias, A., I. M. Miranda, J. Branco, M. Monteiro-Soares, C.
2281 Pina-Vaz et al., 2015 Adhesion, biofilm formation, cell surface
2282 hydrophobicity, and antifungal planktonic susceptibility: rela-
2283 tionship among *Candida* spp. *Front. Microbiol.* 6: 205.
2284 <https://doi.org/10.3389/fmicb.2015.00205>
- 2285 Singh, K., P. J. Kang, and H. O. Park, 2008 The Rho5 GTPase is
2286 necessary for oxidant-induced cell death in budding yeast. *Proc.*
2287 *Natl. Acad. Sci. USA* 105: 1522–1527. <https://doi.org/10.1073/pnas.0707359105>
- 2288 Singh, K., M. E. Lee, M. Entezari, C. H. Jung, Y. Kim et al.,
2289 2019 Genome-wide studies of rho5-interacting proteins that
2290 are involved in oxidant-induced cell death in budding yeast.
2291 *G3 (Bethesda)* 9: 921–931.
- 2292 Smukalla, S., M. Caldara, N. Pochet, A. Beauvais, S. Guadagnini
2293 et al., 2008 FLO1 is a variable green beard gene that drives
2294 biofilm-like cooperation in budding yeast. *Cell* 135: 726–737.
2295 <https://doi.org/10.1016/j.cell.2008.09.037>
- 2296 Sobering, A. K., U. S. Jung, K. S. Lee, and D. E. Levin, 2002 Yeast
2297 Rpi1 is a putative transcriptional regulator that contributes to
2298 preparation for stationary phase. *Eukaryot. Cell* 1: 56–65.
2299 <https://doi.org/10.1128/EC.1.1.56-65.2002>
- 2300 Sohn, K., J. Schwenk, C. Urban, J. Lechner, M. Schweikert et al.,
2301 2006 Getting in touch with *Candida albicans*: the cell wall of a
2302 fungal pathogen. *Curr. Drug Targets* 7: 505–512. <https://doi.org/10.2174/138945006776359395>
- 2303 Song, W., and M. Carlson, 1998 Srb/mediator proteins interact
2304 functionally and physically with transcriptional repressor Sfl1.
2305 *EMBO J.* 17: 5757–5765. <https://doi.org/10.1093/emboj/17.19.5757>
- 2306 Spor, A., S. Wang, C. Dillmann, D. de Vienne, and D. Sicard,
2307 2008 “Ant” and “grasshopper” life-history strategies in *Saccha-*
2308 *romyces cerevisiae*. *PLoS One* 3: e1579. <https://doi.org/10.1371/journal.pone.0001579>
- 2309 Stoldt, V. R., A. Sonneborn, C. E. Leuker, and J. F. Ernst,
2310 1997 Efg1p, an essential regulator of morphogenesis of the
2311 human pathogen *Candida albicans*, is a member of a conserved
2312 class of bHLH proteins regulating morphogenetic processes in
2313 fungi. *EMBO J.* 16: 1982–1991. <https://doi.org/10.1093/emboj/16.8.1982>
- 2314 Taheri, N., T. Kohler, G. H. Braus, and H. U. Mosch,
2315 2000 Asymmetrically localized Bud8p and Bud9p proteins
2316 control yeast cell polarity and development. *EMBO J.* 19:
2317 6686–6696. <https://doi.org/10.1093/emboj/19.24.6686>
- 2318 Takahashi-Nakaguchi, A., K. Sakai, H. Takahashi, D. Hagiwara, T.
2319 Toyotome et al., 2018 *Aspergillus fumigatus* adhesion factors

- 2315 in dormant conidia revealed through comparative phenotypic
 2316 and transcriptomic analyses. *Cell. Microbiol.* 20: e12802.
 2317 <https://doi.org/10.1111/cmi.12802>
- 2318 Tan, Z., M. Hays, G. A. Cromie, E. W. Jeffery, A. C. Scott *et al.*,
 2319 2013 Aneuploidy underlies a multicellular phenotypic switch.
 2320 *Proc. Natl. Acad. Sci. USA* 110: 12367–12372. <https://doi.org/10.1073/pnas.1301047110>
- 2321 Tedford, K., S. Kim, D. Sa, K. Stevens, and M. Tyers,
 2322 1997 Regulation of the mating pheromone and invasive
 2323 growth responses in yeast by two MAP kinase substrates. *Curr.*
 2324 *Biol.* 7: 228–238. [https://doi.org/10.1016/S0960-9822\(06\)00118-7](https://doi.org/10.1016/S0960-9822(06)00118-7)
- 2325 Tkach, J. M., A. Yimit, A. Y. Lee, M. Riffle, M. Costanzo *et al.*,
 2326 2012 Dissecting DNA damage response pathways by analysing
 2327 protein localization and abundance changes during DNA repli-
 2328 cation stress. *Nat. Cell Biol.* 14: 966–976. <https://doi.org/10.1038/ncb2549>
- 2329 Tronchin, G., J. P. Bouchara, V. Annaix, R. Robert, and J. M. Senet,
 2330 1991 Fungal cell adhesion molecules in *Candida albicans*. *Eur.*
 2331 *J. Epidemiol.* 7: 23–33. <https://doi.org/10.1007/BF00221338>
- 2332 Vadaie, N., H. Dionne, D. S. Akajagbor, S. R. Nickerson, D. J. Krysan
 2333 *et al.*, 2008 Cleavage of the signaling mucin Msb2 by the as-
 2334 partyl protease Yps1 is required for MAPK activation in yeast.
 2335 *J. Cell. Biol.* 181: 1073–1081. <https://doi.org/10.1083/jcb.200704079>
- 2336 van der Felden, J., S. Weisser, S. Bruckner, P. Lenz, and H. U.
 2337 Mosch, 2014 The transcription factors Tec1 and Ste12 interact
 2338 with coregulators Msa1 and Msa2 to activate adhesion and mul-
 2339 ticellular development. *Mol. Cell. Biol.* 34: 2283–2293. <https://doi.org/10.1128/MCB.01599-13>
- 2340 Veelders, M., S. Bruckner, D. Ott, C. Unverzagt, H. U. Mosch *et al.*,
 2341 2010 Structural basis of flocculin-mediated social behavior in
 2342 yeast. *Proc. Natl. Acad. Sci. USA* 107: 22511–22516. <https://doi.org/10.1073/pnas.1013210108>
- 2343 Verstrepen, K. J., G. Derdelinckx, H. Verachtert, and F. R. Delvaux,
 2344 2003 Yeast flocculation: what brewers should know. *Appl. Mi-*
 2345 *crobiol. Biotechnol.* 61: 197–205. <https://doi.org/10.1007/s00253-002-1200-8>
- 2346 Ward, M. P., C. J. Gimeno, G. R. Fink, and S. Garrett, 1995 SOK2
 2347 may regulate cyclic AMP-dependent protein kinase-stimulated
 2348 growth and pseudohyphal development by repressing transcrip-
 2349 tion. *Mol. Cell. Biol.* 15: 6854–6863. <https://doi.org/10.1128/MCB.15.12.6854>
- 2350 Wendland, J., 2001 Comparison of morphogenetic networks of
 2351 filamentous fungi and yeast. *Fungal Genet. Biol.* 34: 63–82.
 2352 <https://doi.org/10.1006/fgb.2001.1290>
- 2353 White, M. A., L. Riles, and B. A. Cohen, 2009 A systematic screen
 2354 for transcriptional regulators of the yeast cell cycle. *Genetics*
 2355 181: 435–446. <https://doi.org/10.1534/genetics.108.098145>
- 2356 Wolfe, K. H., and D. C. Shields, 1997 Molecular evidence for an
 2357 ancient duplication of the entire yeast genome. *Nature* 387:
 2358 708–713. <https://doi.org/10.1038/42711>
- 2359 Younes, S., W. Bahman, H. I. Dimassi, and R. A. Khalaf, 2011 The
 2360 *Candida albicans* Hwp2 is necessary for proper adhesion, bio-
 2361 film formation and oxidative stress tolerance. *Microbiol. Res.*
 2362 166: 430–436. <https://doi.org/10.1016/j.micres.2010.08.004>
- 2363 Zahner, J. E., H. A. Harkins, and J. R. Pringle, 1996 Genetic anal-
 2364 ysis of the bipolar pattern of bud site selection in the yeast
 2365 *Saccharomyces cerevisiae*. *Mol. Cell. Biol.* 16: 1857–1870.
 2366 <https://doi.org/10.1128/MCB.16.4.1857>
- 2367 Zeitlinger, J., I. Simon, C. T. Harbison, N. M. Hannett, T. L. Volkert
 2368 *et al.*, 2003 Program-specific distribution of a transcription
 2369 factor dependent on partner transcription factor and MAPK sig-
 2370 naling. *Cell* 113: 395–404. [https://doi.org/10.1016/S0092-8674\(03\)00301-5](https://doi.org/10.1016/S0092-8674(03)00301-5)
- 2371 Zhao, S., J. J. Huang, X. Sun, X. Huang, S. Fu *et al.*, 2018 (1-
 2372 aryloxy-2-hydroxypropyl)-phenylpiperazine derivatives sup-
 2373 press *Candida albicans* virulence by interfering with morpholog-
 2374 ical transition. *Microb. Biotechnol.* 11: 1080–1089. <https://doi.org/10.1111/1751-7915.13307>
- 2375 Zheng, W., H. Zhao, E. Mancera, L. M. Steinmetz, and M. Snyder,
 2376 2010 Genetic analysis of variation in transcription factor bind-
 2377 ing in yeast. *Nature* 464: 1187–1191. <https://doi.org/10.1038/nature08934>
- 2378 Zhou, H., and F. Winston, 2001 NRG1 is required for glucose
 2379 repression of the SUC2 and GAL genes of *Saccharomyces cere-
 2380 visiae*. *BMC Genet.* 2: 5. <https://doi.org/10.1186/1471-2156-2-5>
- 2380 Zhou, W., M. W. Dorrrity, K. L. Bubb, C. Queitsch, and S. Fields,
 2381 2020 Binding and regulation of transcription by yeast Ste12
 2382 variants to drive mating and invasion phenotypes. *Genetics* 214:
 2383 397–407. <https://doi.org/10.1534/genetics.119.302929>

Communicating editor: A. Gladfelter

Do you want to participate in the Author's Choice Open Access option for your article?

- No 
- Yes, Standard Open Access
- Yes, Creative Commons CC BY 4.0 License

Both Author Choice Open options make your article freely available to all readers (regardless of subscription) immediately after publication. With the Standard Author Choice Open Access, copyright remains with the Genetics Society of America as outlined in our copyright policy and future re-use of your content by others requires permission from GSA. With the CC BY 4.0 option, you hold copyright on the article, but anyone can share or adapt for any purpose, even commercially so long as they attribute the original source. Some authors have explained that they do not wish to grant others the right to modify and/or sell their content, so we offer both choices for the content to be made freely-available. Both Open Access options carry a surcharge of \$1500 for GSA members or \$2000 for non-members

More information: <http://www.genetics.org/content/after-acceptance#charges>

[QAI] If you or your coauthors would like to include an ORCID ID in this article, please provide your respective ORCID IDs along with your corrections.

Note: If you do not yet have an ORCID ID and would like one, you may register for this unique digital identifier at <https://orcid.org/register>.

- [1]** Please check the *Saccharomyces* Genome Database links throughout.
- [2]** Please verify the affiliations are correct.
- [3]** Please confirm the corresponding author's address.
- [4]** Please check all figure legends carefully to confirm that any and all labels, designators, directionals, colors, etc. are represented accurately in comparison with the figure images.
- [5]** Any alternations between capitalization and/or italics in genetic and taxonomic nomenclature have been retained per the original manuscript. *Genetics* style is for genes and alleles to be italicized; please confirm that all nomenclature has been formatted properly throughout. Per journal style, uppercase Greek letters should remain roman even when appearing in a term where the overall style is italic (e.g., a gene name such as *kap108Δ*). Note that headings are set all roman or all italics based on journal style and should not be changed. 
- [6]** Please verify all URLs in your article.
- [7]** If you or your coauthors provided an ORCID ID, please verify the accuracy of the ID number(s) on the proof as presented. If you or your coauthors would like to include an ORCID ID in this article, please provide your respective ORCID IDs along with your corrections. Note: If you do not yet have an ORCID ID and would like one, you may register for this unique digital identifier at <https://orcid.org/register>.
- [8]** A required subsection at the end of the Materials and Methods entitled "Data availability" has been added per journal style. Please confirm that this statement is accurate, or if not, update to include the details of where your data can be found. Details are available in the Materials and Methods instructions at <http://www.genetics.org/content/prep-manuscript#text>.